Published for SISSA by Springer

Received: *August 21, 2016*
Accepted: *September 23, 2016*
Published: *October 6, 2016*

Cutkosky rules for superstring field theory

Roji Pius[a] **and Ashoke Sen**[b]

[a] *Perimeter Institute for Theoretical Physics, Waterloo, ON N2L 2Y5, Canada*
[b] *Harish-Chandra Research Institute, Chhatnag Road, Jhusi, Allahabad 211019, India*

E-mail: rpius@perimeterinstitute.ca, sen@mri.ernet.in

Abstract: Superstring field theory expresses the perturbative S-matrix of superstring theory as a sum of Feynman diagrams each of which is manifestly free from ultraviolet divergences. The interaction vertices fall off exponentially for large space-like external momenta making the ultraviolet finiteness property manifest, but blow up exponentially for large time-like external momenta making it impossible to take the integration contours for loop energies to lie along the real axis. This forces us to carry out the integrals over the loop energies by choosing appropriate contours in the complex plane whose ends go to infinity along the imaginary axis but which take complicated form in the interior navigating around the various poles of the propagators. We consider the general class of quantum field theories with this property and prove Cutkosky rules for the amplitudes to all orders in perturbation theory. Besides having applications to string field theory, these results also give an alternative derivation of Cutkosky rules in ordinary quantum field theories.

Keywords: String Field Theory, Superstrings and Heterotic Strings

ArXiv ePrint: 1604.01783

doi:10.1007/JHEP10(2016)024

JHEP10(2016)024

Contents

JHEP10(2016)024

1 Introduction

Unitarity is a necessary property of any theory that aims at describing the fundamental constituents of matter and their interactions. Since superstring theory is, at present, the leading candidate for such a theory, it is necessary to ensure that the scattering matrix computed from superstring theory is unitary. The goal of this paper will be to address this issue in superstring perturbation theory.

Our strategy will be to make use of superstring field theory[1] — a quantum field theory whose Feynman rules reproduce the perturbative amplitudes computed using the conven-

[1]Our analysis will not require using any specific version of superstring field theory. For definiteness we can consider the version of quantum superstring field theory considered in [1]. Most of the other recent work has been towards the construction of classical open and/or closed superstring field theory [2–20]. If they can be elevated to consistent quantum theory, they may provide equally good candidates for our analysis. One may also be able to use non-local versions of closed superstring field theory of the kind suggested in [21].

tional Polyakov approach. The advantage of using superstring field theory is that we can use the well known techniques of quantum field theory to address various issues. In particular one might expect that the conventional approach to proving unitarity of quantum field theories using Cutkosky rules [22–26] may be used to give a proof of unitarity of superstring perturbation theory, since these rules encode the perturbation expansion of the relation $S^\dagger S = 1$ satisfied by the S-matrix S.

It turns out however that there is one way in which superstring field theory differs from conventional quantum field theories. The interaction vertices of superstring field theory have the property that they fall off exponentially when the external states carry large space-like momenta. This property is what makes the superstring perturbation expansion manifestly free from ultraviolet divergences. However there is a flip side to this story — for large time-like momenta the interaction vertices diverge exponentially. For this reason, the only way to make sense of integration over loop energies is to let the energy integration contours reach infinity along the imaginary axis. If we consider the Wick rotated Green's function in which all the external states carry imaginary energy, this is straightforward. We simply take all the loop energy integrals to lie along the imaginary axis so that all the propagators and vertices carry imaginary energy. This leads to non-singular integrand with exponential fall-off at infinity and the integral is well defined. In a conventional quantum field theory, we could inverse Wick rotate[2] all the external energies towards the real axis and at the same time rotate the energy integration contours clockwise from the imaginary axis to the real axis, eventually arriving at the formalism where the energies of external states are real, and the loop energy integrals run along the real axis with $i\epsilon$ prescription for dealing with the poles of the propagator. However such an integral will be ill defined in string field theory, since the vertex factors will blow up exponentially as the loop energy integrals approach infinity along the real axis. For this reason, even when we inverse Wick rotate the external energies from the imaginary axis back to the real axis, we must continue to let the loop energy integration contours reach infinity along the imaginary axis. However we can no longer ensure that these integrals run all along the imaginary axis since during the inverse Wick rotation of external energies, some of the poles of the propagator will approach the imaginary energy axis and we have to deform the integration contour away from these poles in order to ensure that we get the analytic continuation of the Wick rotated result. As a result, when the external energies reach the real axis, we typically will have a complicated integration contour over the loop energies with their ends tied at $\pm i\infty$. For example for the one loop amplitude shown in figure 1 in page 11, a possible integration contour over the loop energy is shown in figure 3 in page 13.

Since the proof of unitarity involves identifying the anti-hermitian part of the amplitude, we now have to identify the anti-hermitian part of this Feynman integral. *A priori* the result looks complicated due to the fact that the choice of integration contour does not have simple reality properties. One can in fact show that the prescription for computing the hermitian conjugate of the T-matrix reduces to the computation of a Feynman integral similar to the original integral, with all the external energies replaced by their complex con-

[2]In our notation, Wick rotation will denote taking the energies from the real axis to the imaginary axis, while inverse Wick rotation will correspond to taking them from the imaginary axis to the real axis.

JHEP10(2016)024

jugates and the integration contour over the loop energies related to the original contour by complex conjugation. The main result of this paper involves proving that to all orders in perturbation theory, this difference between the two integrals is given by Cutkosky rules in the limit when the external energies approach the real axis.

If we denote by T the T-matrix related to the S-matrix via the relation $S = 1 - iT$, then Cutkosky rules express the difference between T and its hermitian conjugate $T^\dagger$ as a sum of cut Feynman diagrams in which we draw an oriented line through the Feynman diagrams contributing to the original T-matrix, dividing the diagram into two pieces. In every cut propagator, the original propagator is replaced by the product of a delta function that sets the momentum along the propagator on-shell and a step function that forces the energy of the propagator to flow from the left to the right of the cut. The contribution from part of the Feynman diagram to the left of the cut is computed using the usual Feynman rules and the contribution from part of the Feynman diagram to the right of the cut is given by the hermitian conjugate of the corresponding Feynman diagram. The contributions from the cut diagrams have the interpretation of the matrix elements of $T^\dagger T$, computed by inserting a complete set of states between $T^\dagger$ and T represented by the cut propagators. After taking into account the factors of i we arrive at the relation $T - T^\dagger = -iT^\dagger T$, which is precisely the statement of unitarity of the S-matrix.

In quantum field theories where all the fields represent fundamental particles, the Cutkosky rules establish the unitarity of the S-matrix. For theories with local gauge symmetry, including string field theory, Cutkosky rules are necessary ingredients for the proof of unitarity, but they are not sufficient. These theories contain many unphysical and pure gauge states besides physical states, and we must show that only the physical states contribute to the sum over intermediate states. In conventional gauge theories this is proved using Ward identities (see e.g. [25]). Since gauge invariance of string theory leads to similar Ward identities [27], we expect that they can be used to complete the proof of unitarity. We leave this for future work.

The paper is organized as follows. In section 2 we introduce a toy scalar field theory that captures all the essential properties of string field theory that goes into the proof of Cutkosky rules. In order to define an amplitude in this theory with Lorentzian external momenta, with the s-th external particle carrying spatial momenta $\vec{p}_s$ and energy E_s, we begin with an amplitude where the s-th particle has spatial momenta $\vec{p}_s$ and energy λE_s, where λ is a complex parameter. For purely imaginary λ the amplitude is defined by taking all the loop energy integrals along the imaginary axis. We then define the physical amplitude, corresponding to $\lambda = 1$, by analytic continuation of the result on the imaginary λ-axis to the real λ-axis *via the first quadrant of the complex λ-plane.* In section 4 we prove that this analytic continuation procedure is well defined by showing that the amplitude does not have any singularity in the first quadrant of the λ-plane. In section 2 we also derive an algorithm for computing the hermitian conjugate of an amplitude.

In section 3 we consider a simple one loop amplitude in this theory and show how Cutkosky rules hold for this amplitude. The complete proof to all orders in perturbation theory is carried out in section 5. This is done in several steps. First we show that for fixed values of the spatial components of loop momenta the contribution to the anti-hermitian

JHEP10(2016)024

part of a connected amplitude is non-vanishing only when some of the integration contours over the loop energy integrals are pinched, i.e. two poles approach each other from opposite sides of a contour so that we cannot deform the contour away from the poles without passing through a pole. Then we divide the contribution from the pinch singularities into two classes, one vertex irreducible (1VI) diagram and one vertex reducible (1VR) diagrams, and show that Cutkosky rules hold for the 1VR diagrams as long as they hold for the 1VI diagrams. Next we prove the Cutkosky rules for 1VI diagrams. Finally we prove that the Cutkosky rules for disconnected diagrams follow as a consequence of the Cutkosky rules for connected diagrams. Our proof uses the method of induction in the number of loops, and holds to all orders in perturbation theory.

In section 6 we describe how the analysis of the toy model in the previous sections captures most, but not all, of the ingredients needed to prove unitarity of superstring field theory. We discuss what else needs to be done to prove the unitarity of superstring perturbation theory. Some of these are common to ordinary quantum field theories, e.g. we need to work in sufficiently high dimensions so that we avoid the usual infrared divergence problems that plague quantum field theories in dimensions ≤ 4, and we need to prove the cancellation of the contributions from intermediate unphysical and pure gauge states using Ward identities. However some of them are purely technical problems in string field theory — e.g. proving the reality of the superstring field theory action — which we believe can be proven with some effort but has not been done so far.

We conclude this introductory section by reviewing some of the previous work on this subject. A complete proof of unitarity of superstring perturbation theory was attempted in [28] by showing the equivalence of the perturbative amplitudes in superstring theory and the amplitudes in light-cone string field theory. Since the latter is manifestly unitary, this would imply unitarity of the S-matrix computed in the covariant formulation. In view of recent understanding of the subtleties of superstring perturbation theory [29–32] one should reinvestigate this correspondence. Nevertheless it seems quite likely that this will lead to a concrete formulation of light-cone string field theory which will still be manifestly unitary and at the same time generate the usual amplitudes of perturbative superstring theory. This would establish the unitarity of perturbative superstring amplitudes. However the main advantage of using a covariant superstring field theory for our analysis is that this theory can be used to analyze unitarity and other properties of string theory not only in the perturbative vacuum, but also in situations where loop corrections require us to shift the vacuum expectation values of the fields away from that in the perturbative vacuum [27]. The shift in the field will change the vertices, but not their general properties on which we shall base our analysis as long as the string field theory action in the shifted background continues to be real.

One could also try to prove the unitarity of superstring perturbation theory directly by using the $i\epsilon$ prescription for defining the perturbative amplitudes as given in [33, 34]. At this stage it is not known how this can be done, but it is conceivable that one can translate this $i\epsilon$ prescription into a direct proof of unitarity of the perturbative superstring amplitudes. However this will still suffer from the fact that the proof will not extend in a straightforward manner to the cases where the true vacuum is related to the perturbative vacuum by a shift in the fields.

JHEP10(2016)024

Finally we would like to add one word about convention. Throughout this paper we shall use the notion of a pinch singularity to denote that the integration contours over some loop energies encounter poles approaching each other from opposite sides of the contours so that by deforming the contours into the complex loop energy plane we cannot avoid these poles. However we shall always keep the integration over the spatial components of loop momenta along the real axes. This notion differs from that used in the standard literature e.g. in [22, 23], where a contour is declared to be pinched only if it cannot be deformed away from the pole by deforming the integration contour into the complex energy and / or complex spatial momentum plane. Due to this, some of our results, e.g. that the anti-hermitian part of the amplitude comes only from pinch singularities, may look unfamiliar to the experts. On the other hand, our approach leads to a proof of the Cutkosky rules at fixed values of the spatial components of the loop momenta and for general off-shell external states. This is close in spirit to the results of [35], although the analysis of [35] cannot be applied directly to the class of field theories we consider due to essential singularities of the interaction vertices at infinite momenta.

2 The field theory model

In this section we shall introduce a toy quantum field theory that captures all the essential features of the subtleties of string field theory action. Our model will involve a single scalar field. But the analysis we shall perform can be easily generalized to the case of multiple fields including fields of higher spin, since Lorentz invariance will not play any significant role in our analysis. In section 6 we shall discuss what additional subtleties we need to address in order to translate the result of this paper to a complete proof of unitarity of superstring field theory.

2.1 The model

We consider a scalar field theory in $(d+1)$-dimensions containing a single real scalar field ϕ, with the following action written in momentum space:

$$\begin{aligned} S = & -\frac{1}{2}\int \frac{d^{d+1}k}{(2\pi)^{d+1}}\phi(-k)(k^2+m^2)\phi(k) \\ & -\sum_n \frac{1}{n!}(2\pi)^{-(n-1)(d+1)}\int d^{d+1}k_1\cdots d^{d+1}k_n\,\delta^{(d+1)}(k_1+\cdots+k_n) \\ & \qquad\qquad \times V^{(n)}(k_1,\cdots k_n)\,\phi(k_1)\cdots\phi(k_n)\,. \end{aligned} \tag{2.1}$$

Here $k^2 \equiv -(k^0)^2+(k^1)^2+\cdots+(k^d)^2$, $d^{d+1}k \equiv dk^0dk^1\cdots dk^d$ and the vertices $V^{(n)}$ satisfy the reality condition

$$(V^{(n)}(k_1,\cdots k_n))^* = V^{(n)}(-k_1^*,\cdots -k_n^*)\,, \tag{2.2}$$

where $*$ denotes complex conjugation. We take the $V^{(n)}$'s to be invariant under arbitrary permutation of the arguments, and assume that they have no singularities in the k_s^μ planes at finite values. Furthermore, they vanish exponentially as one or more k_s^0 approach $\pm i\infty$

JHEP10(2016)024

along the imaginary axis and/or one or more k_s^i for $1 \le i \le d$ approach $\pm\infty$ along the real axis, keeping the other k_r's fixed. On the other hand, $V^{(n)}$ may blow up exponentially as k_s^0 and/or k_s^i approach infinity in certain other directions, e.g. along the real k_s^0 axis or the imaginary k_s^i axis. Therefore $V^{(n)}$'s have essential singularities at infinity.

Note that due to the exponential growth of $V^{(n)}$ for large time-like momentum, a classical field configurations $\phi(k)$ with real argument $\{k^\mu\}$ will have finite action only if it falls off sufficiently fast for large $|k^0|$ so as to compensate for the exponential growth of the $V^{(n)}$'s. Once this condition is satisfied and the action is finite, then (2.1) is real for real field configuration satisfying $\phi(k)^* = \phi(-k)$. We shall of course not be interested in classical field configirations — for us the significance of (2.1) lies in the fact that this is the property that we expect the superstring field theory action to possess.

The Feynman rules for computing the T-matrix, related to the S-matrix via $S = I - i\,T$, are as follows:

$$\begin{aligned}
\text{propagator of momentum } k &: -i\,(k^2+m^2)^{-1} \\
n\text{-point vertex with incoming momenta } k_1,\cdots k_n &: -i\,V^{(n)}(k_1,\cdots k_n) \\
\text{each loop momentum integration} &: \frac{d^{d+1}\ell}{(2\pi)^{d+1}} \\
\text{overall factor} &: i\,(2\pi)^{d+1}\delta^{(d+1)}\left(\sum_s p_s\right)\,,
\end{aligned} \tag{2.3}$$

where in the last equation the sum over s runs over all the external momenta p_s in the convention that p_s denotes the momentum entering the diagram from outside. If the diagram has disconnected components then there will be separate momentum conserving delta function for each component. These rules are derived from path integral expressions for the Green's functions with weight factors e^{iS}.

We can simplify the Feynman rules somewhat by extracting a factor of i from each propagator, a factor of $-i$ from each vertex and the overall factor of i given in the last line of (2.3). This gives a total factor of $(i)^{n_p-n_v+1}$ where n_p is the number of propagators and n_v is the number of vertices. If n_ℓ is the number of loops, then using the relation

$$n_\ell = n_p - n_v + 1\,, \tag{2.4}$$

that holds for a connected diagram, we get a net factor of

$$(i)^{n_p-n_v+1} = (i)^{n_\ell}\,. \tag{2.5}$$

If the diagram has n_c disconnected components then (2.4) will be replaced by $n_\ell = n_p - n_v + n_c$, and hence the net factor given in the right hand side of (2.5) will be

$$(i)^{n_\ell-n_c+1}\,. \tag{2.6}$$

For now we shall proceed by assuming that the diagram is connected so that (2.5) holds. Therefore each loop integral is accompanied by a factor of i. The modified Feynman rules

JHEP10(2016)024

now involve

$$\begin{aligned}\text{propagator of momentum } k : P(k) &= -(k^2+m^2)^{-1} \\ &= \left(k^0 - \sqrt{\vec{k}^2+m^2}\right)^{-1}\left(k^0 + \sqrt{\vec{k}^2+m^2}\right)^{-1} \\ \text{vertex with incoming momenta } k_1,\cdots k_n &: V^{(n)}(k_1,\cdots k_n) \\ \text{each loop momentum integration} &: i\,\frac{d^{d+1}\ell}{(2\pi)^{d+1}} \\ \text{overall factor} &: (2\pi)^{d+1}\delta^{(d+1)}\left(\sum_k p_k\right) . \end{aligned} \tag{2.7}$$

Since the vertices diverge exponentially for large time-like external momenta, individual Feynman diagrams in this theory have somewhat strange properties. For example the s-channel diagram for a tree level 4-point function, in which a pair of 3-point functions are joined by a single internal propagator, will blow up exponentially in the limit of large center of mass energy of the incoming particles. In string field theory this effect is cancelled by the contribution from the 4-point vertex. On the other hand, this property of the vertices makes the individual Feynman diagrams manifestly free from ultraviolet divergences once we choose the loop momentum integration contours appropriately. This will be described in the next subsection.

2.2 Loop momentum integration contours

Due to the peculiar behavior of the interaction vertices at large momenta, the integration over loop momenta has to be defined somewhat carefully. The integrals over $\vec{\ell}_k \equiv (\ell_k^1, \cdots \ell_k^d)$ — the spatial components of the loop momenta — are taken to be along the real axis, but the integration contours for the ℓ_k^0's — the zeroth components of all the loop momenta — are chosen as follows. Let us denote collectively by $\{p_s^0\}$ the zero components of the external momenta $\{p_s\}$. We shall introduce a set of numbers $\{E_s\}$ which denote the actual real values of the $\{p_s^0\}$ for which we want to compute the Green's function, and consider a more general set of external momenta where $p_s^0 = \lambda E_s$ with λ an arbitrary complex number. When λ is purely imaginary then we can get a well-defined expression for the Green's function by taking the integration contour for ℓ_k^0's to run along the imaginary axis. In this case all the internal propagators carry imaginary energy and real spatial momenta and hence are free from singularities. Furthermore since the ℓ_k^0 integration contour approaches infinity along the imaginary axis and the $\ell_k^1, \cdots \ell_k^d$ integration contours approach infinity along the real axis, we get a convergent loop momentum integral due to the convergence property of $V^{(n)}$ discussed above. We now define the off-shell Green's function for general λ as the analytic continuation of this expression in the complex λ plane. Operationally this means that as we deform λ away from the imaginary axis, we continue to define the Green's function by taking the integration contour over ℓ_k^0's to run from $-i\infty$ to $i\infty$ till some pole of the integrand approaches the imaginary ℓ_k^0 axis. When a pole approaches the imaginary ℓ_k^0 axis, we deform the integration contour away from the imaginary axis to avoid the poles, keeping its ends fixed at $\pm i\infty$. The integrations over the spatial components

JHEP10(2016)024

of loop momenta are always taken to be along the real axis.[3] We shall show in section 4 that the off-shell Green's function defined this way is an analytic function of λ in the first quadrant of the complex plane, i.e. for $\mathrm{Re}(\lambda) \geq 0$, $\mathrm{Im}(\lambda) > 0$. This is simply the statement that as long as λ remains in the first quadrant, a deformation of the integration contour of the kind mentioned above is always possible. For any amplitude, we shall denote by C the collective prescription for all the ℓ_k^0 integration contours.

As is well known, if the integrands had sufficiently rapid fall off as $\ell_k^0 \to \infty$ in any direction in the complex plane, the above prescription is equivalent to the usual $i\epsilon$ prescription for computing Green's functions. To see this let us replace m^2 by $m^2 - i\epsilon$ in the propagators. Since the euclidean path integral has no divergences, in the $\epsilon \to 0^+$ limit this replacement has no effect on the Euclidean Green's functions with $p_s^0 = iE_s$. Now we rotate each external p_s^0 from imaginary to real axis by taking $p_s^0 = E_s e^{i\theta}$ and letting θ vary from $\pi/2$ to 0. We can accompany this by a deformation of the integration contour over ℓ_k^0's by replacing ℓ_k^0 by $e^{i\theta} u_i$ with real u_i. As long as the integrand falls off sufficiently fast as $\ell_k^0 \to \pm e^{i\theta} \times \infty$, this is an allowed deformation of the contour. During this deformation the momentum $k_j \equiv (k_j^0, \vec{k}_j)$ flowing through the j-th internal propagator will take the form $(e^{i\theta}\kappa_j, \vec{k}_j)$ with real κ_j. Therefore we have

$$k_j^2 + m^2 - i\epsilon \equiv -(k_j^0)^2 + \vec{k}_j^2 + m^2 - i\epsilon = -\kappa_j^2 e^{2i\theta} + \vec{k}_j^2 + m^2 - i\epsilon\,. \tag{2.8}$$

For $\epsilon > 0$ and $0 \leq \theta \leq \pi/2$ this has strictly negative imaginary part and hence does not vanish. Therefore the deformed contour does not cross any pole as we vary θ from $\pi/2$ to 0. For $\theta = \pi/2$ this gives the euclidean expression whereas for $\theta = 0$ we get the usual Feynman rules with Lorentzian momentum integration with the $i\epsilon$ prescription.

Of course for the kind of vertices we are using here this rotation of the integration contours is not allowed due the essential singularity that the integrand has at infinity. Therefore we have to work with the integration contour with the end-points of ℓ_k^0 contour integrals fixed at $\pm i\infty$, as mentioned above. Nevertheless, replacing m^2 by $m^2 - i\epsilon$ serves a useful purpose of determining which side of the integration contour a given singularity lies. For this let us express the propagator $-(k^2+m^2)^{-1}$ as $\left(k^0 - \sqrt{\vec{k}^2 + m^2}\right)^{-1}\left(k^0 + \sqrt{\vec{k}^2 + m^2}\right)^{-1}$. In this case if we replace m^2 by $m^2 - i\epsilon$ and pretend that the k^0 integral runs along the real axis towards $+\infty$, then the first pole lies to the right of the k^0 integration contour whereas the second pole lies to the left of the integration contour. This property is inherited from the original definition of the integral for purely imaginary λ where the k^0 integral runs along the imaginary axis from $-i\infty$ to $i\infty$, and must be satisfied by the k^0 integration contour for any λ in the first quadrant. Therefore the $i\epsilon$ prescription may be regarded as a way of keeping track of on which side of the integration contour a pole lies, — we simply

[3] This prescription is not manifestly Lorentz invariant, since the standard proof of Lorentz invariance requires us to transform the loop momenta by the same Lorentz transformation that acts on the external states, and this does not leave the end points of the contour invariant. However the new contour obtained by Lorentz transformation will also have the property that the integrand falls off exponentially at the two ends since the integrand is manifestly Lorentz invariant. As a result we can prove the equality of the new integral with the old integral by deforming the new contour to the old one near the end points by successive infinitesimal Lorentz transformations.

JHEP10(2016)024

have to pretend that the k^0 integration runs along the real axis towards $+\infty$, and read off which side of the contour the pole is on when we replace m^2 by $m^2 - i\epsilon$.

2.3 Hermitian conjugate of the T-matrix

The Feynman rules described above directly compute the T-matrix. Our goal will be to compute the difference $\langle a|(T - T^\dagger)|b\rangle$ for incoming states $|b\rangle$ and outgoing states $\langle a|$. For this we use the relation[4]

$$\langle a|T^\dagger|b\rangle = \langle b|T|a\rangle^* \,, \tag{2.9}$$

and proceed as follows:

1. We use the Feynman rules to compute the right hand side of (2.9). Now in our convention where all external states have their momenta entering the Feynman diagram, an external line of momentum p_i with positive p_i^0 is to be interpreted as an incoming state of $(d+1)$-momentum p_i whereas an external state of momentum p_i with negative p_i^0 is to be interpreted as an outgoing state of $(d+1)$-momentum $-p_i$. Therefore $\langle b|T|a\rangle$ can be obtained from $\langle a|T|b\rangle$ by simply switching the signs of all the external momenta.

2. Due to the change in sign of the external momenta, the ℓ_k^0 integration contours for computation of $\langle b|T|a\rangle$ will have to be deformed in a way that is different from what we have for $\langle a|T|b\rangle$, since the poles are at different places. However if we make a change of variables in which each loop momentum ℓ_k is replaced by $-\ell_k$ then all the momenta carried by the internal vertices and propagators[5] in the expression for $\langle b|T|a\rangle$ will have their signs reversed compared to the integrand appearing in the computation of $\langle a|T|b\rangle$. Since this does not change the positions of the poles, the contours for $\langle b|T|a\rangle$ can now be defined in the same way as for $\langle a|T|b\rangle$. The $(-1)^{d+1}$ factor picked up by the measure $d^{d+1}\ell_k$ during the change of variables is compensated by an orientation reversal of the integration contours, so that each ℓ_k^i integral for $1 \le i \le d$ still runs from $-\infty$ to ∞ along the real axis and each ℓ_k^0 integration still runs from $-i\infty$ to $i\infty$ along the original contour. This shows that $\langle b|T|a\rangle$ can be computed by taking the expression for $\langle a|T|b\rangle$ and changing the sign of the arguments of each vertex factor $V^{(n)}$ and internal propagator that appears in the amplitude, keeping the integration contours unchanged.

3. Next we study the effect of the complex conjugation appearing on the right hand side of (2.9). This changes the factor of i accompanying each ℓ_k^0 integral to $-i$, and complex conjugates all the vertices and propagators. We can now use (2.2) and the minus signs in the arguments of $V^{(n)}$ introduced at the previous step to bring the factors of $V^{(n)}$ back to the form in which they appeared in the expression for $\langle a|T|b\rangle$, except that their arguments are replaced by their complex conjugates. On the other hand in each propagator factor the momentum gets complex conjugated. Therefore

[4] We use the shorthand notation $\langle a|S|b\rangle \equiv \langle a, \text{out}|b, \text{in}\rangle$ and $\langle a|S^\dagger|b\rangle \equiv \langle a, \text{in}|b, \text{out}\rangle$.

[5] The change in sign of the momentum does not affect the propagator, but we have included it to facilitate generalizations in section 6.

JHEP10(2016)024

the net difference between the expressions for $\langle a|T|b\rangle$ and $\langle b|T|a\rangle^*$ is that all the momentum factors in the integrand are replaced by their complex conjugates and the factor of i accompanying each loop integral is replaced by $-i$.

4. If we make a further change in the variables $\ell_k^0 \to (\ell_k^0)^*$, it sends the integrand for $\langle b|T|a\rangle^*$ to its original form that appears in the computation of $\langle a|T|b\rangle$ except that all the external momenta are replaced by their complex conjugates. The new ℓ_k^0 contour would run from $i\infty$ to $-i\infty$, but we compensate for this by changing its orientation by absorbing the $-$ sign from the factor of $-i$ mentioned at the end of the last paragraph. However the new contours now are related to the original contours by complex conjugation. We denote the new choice of contours collectively by C^*. An example of how C^* is constructed from C can be found in section 3 (see figure 3) and a systematic procedure for constructing C and C^* will be described in section 4.2.

5. As long as the contours can be kept away from the poles, we can take the limit in which the external energies approach real values. In that case the integrands in the expressions for $\langle a|T|b\rangle$ and $\langle b|T|a\rangle^*$ become identical. We shall see however that this is not always possible since the contours may encounter pinch singularities in this limit. In such cases we have to take the limit after carrying out the integration.

To summarize, we have shown that the expression for $\langle a|T^\dagger|b\rangle$ takes a form similar to that for $\langle a|T|b\rangle$, except that in the integrand the external momenta are replaced by their complex conjugates and the choice of integration contours over ℓ_k^0, denoted collectively by C, is replaced by C^*. Therefore the difference between T and $T^\dagger$ can be computed by calculating the difference between these two contour integrals. Our goal will be to prove that this difference is given by the Cutkosky rules. In carrying out this analysis we shall make use of the freedom of deforming the ℓ_k^0 contours in the complex ℓ_k^0 plane, possibly picking up residues from the poles that the contour crosses, but keep the ends of the integration contour always tied at $\pm i\infty$ to ensure convergence of the integral.

3 One loop four point function

In this section we shall analyze in detail the simple example of a contribution to the four point function shown in figure 1. Using (2.7) the contribution to the Green's function is given by

$$A(p_1,p_2,p_3,p_4) = i\int_C \frac{d^{d+1}\ell}{(2\pi)^{d+1}}\{(\ell^0)^2-\vec{\ell}^2-m^2\}^{-1}\{(p^0-\ell^0)^2-(\vec{p}-\vec{\ell})^2-m^2\}^{-1} \times V^{(4)}(p_1,p_2,-\ell,\ell-p)\,V^{(4)}(\ell,p-\ell,p_3,p_4)\,. \tag{3.1}$$

We have dropped the overall factor of $(2\pi)^{d+1}\delta^{(d+1)}(p_1+p_2+p_3+p_4)$ to avoid cluttering, and C denotes the integration contour as described in section 2. Following the logic described

JHEP10(2016)024

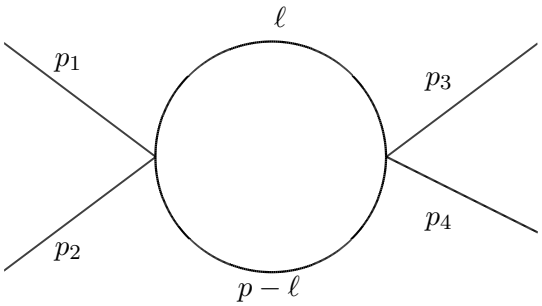

Figure 1. A one loop contribution to the four point function. All external momenta flow inwards, the internal momenta ℓ and $p-\ell$ flow from left to right and $p = p_1 + p_2 = -(p_3 + p_4)$.

at the end of section 2 we also get, after some change of variables,

$$A(-p_1,-p_2,-p_3,-p_4)^* = i\int_{C^*}\frac{d^{d+1}\ell}{(2\pi)^{d+1}}\{(\ell^0)^2-\vec{\ell}^2-m^2\}^{-1}\{((p^0)^*-\ell^0)^2-(\vec{p}-\vec{\ell})^2-m^2\}^{-1} \times V^{(4)}(p_1^*,p_2^*,-\ell,\ell-p^*)\,V^{(4)}(\ell,p^*-\ell,p_3^*,p_4^*)\,, \tag{3.2}$$

where C^* is the contour obtained from C after complex conjugation and an orientation reversal so that it still runs from $-i\infty$ to $i\infty$. Therefore $A(p_1,p_2,p_3,p_4)$ and $A(-p_1,-p_2,-p_3,-p_4)^*$ differ from each other only in the choice of the integration contour, and complex conjugation of the external momenta.

Let us return to (3.1). The poles in the ℓ^0 plane are at

$$Q_1 \equiv \sqrt{\vec{\ell}^2+m^2},\quad Q_2 \equiv -\sqrt{\vec{\ell}^2+m^2},\quad Q_3 \equiv p^0+\sqrt{(\vec{p}-\vec{\ell})^2+m^2},\quad Q_4 \equiv p^0-\sqrt{(\vec{p}-\vec{\ell})^2+m^2}. \tag{3.3}$$

Let E_s's be the physical real values of p_s^0 that we are interested in, and define $E \equiv E_1+E_2 = -(E_3+E_4)$. Let us for definiteness take E_1, E_2 to be positive and E_3, E_4 to be negative so that E is positive. This corresponds to choosing p_1 and p_2 as incoming momenta and $-p_3$ and $-p_4$ as outgoing momenta. In order that this amplitude can be defined via analytic continuation from the Euclidean result as suggested in section 2, we have to ensure that for $p_s = \lambda E_s$ the amplitude defined above has no singularity for λ in the first quadrant. This in the present circumstances correspond to $p^0 = \lambda(E_1+E_2)$ lying in the first quadrant. Now our prescription for defining the Green's function for p^0 on the imaginary axis is to take the integration contour of ℓ^0 from $-i\infty$ to $i\infty$ along the imaginary axis. In this case the poles Q_2 and Q_4 are to the left of the integration contour and the poles Q_1 and Q_3 are to the right of the integration contour. As p^0 moves into the first quadrant, the positions of the poles shift. If they come towards the imaginary ℓ^0 axis, then analytic continuation of the original results is obtained by deforming the ℓ^0 integration contour into the complex plane to avoid the pole, keeping its ends fixed at $\pm i\infty$. We shall hit a singularity in the p^0-plane if the singularity is pinched, i.e. two poles approach the same point on the integration contour from opposite sides so that we cannot deform the contour away from the pole without passing through one of the poles. In the present context this would happen if Q_2 approaches Q_1 or Q_3, or Q_4 approaches Q_1 or Q_3. Now from the expressions given in (3.3)

JHEP10(2016)024

it is clear that for real $\vec{\ell}$, Q_1 cannot approach Q_2 and Q_3 cannot approach Q_4. Therefore the only possibilities are Q_2 approaching Q_3 or Q_4 approaching Q_1. The conditions for these to happen can be written as

$$p^0 = \pm \left(\sqrt{\vec{\ell}^2 + m^2} + \sqrt{(\vec{p} - \vec{\ell})^2 + m^2} \right) . \tag{3.4}$$

Since the right hand side of (3.4) is real, this can be avoided as long as p^0 is away from the real axis. This shows that the amplitude is free from singularities as long as p^0 lies in the first quadrant, and we can define the amplitude for real positive p^0 by taking the $\mathrm{Im}(p^0) \to 0$ limit from above. An alternative but equivalent approach will be to replace m^2 by $m^2 - i\epsilon$. In this case the right hand sides of (3.4) will lie in the fourth and the second quadrants. Therefore as p^0 approaches a positive real value from the first quadrant, the analyticity property of the integral extends all the way up to real p^0 axis, and we can define the amplitude for real p^0 by taking the $\epsilon \to 0^+$ limit after setting p^0 to be real.

The story can be repeated even in the case $E < 0$. In this case $p^0 = \lambda E$ lies in the third quadrant and the possible solution to (3.4) comes from the choice of minus sign on the right hand side. This can be avoided as long as $\mathrm{Im}(p^0) < 0$, i.e. $\mathrm{Im}(\lambda) > 0$, and we define the amplitude for real negative p^0 by taking $\mathrm{Im}(p^0) \to 0$ from below. Alternatively, replacing m^2 by $m^2 - i\epsilon$ shifts the right hand side of (3.4) with the choice of minus sign to the second quadrant. Therefore the analyticity property of the integral also holds when we consider real negative p^0, i.e. real positive λ. This allows us to take p^0 to be real keeping $\epsilon > 0$ and then take $\epsilon \to 0^+$ limit.

This proves the desired analyticity property of the Green's function that allows us to define the amplitudes for real p^0 via analytic continuation of the amplitude for imaginary p^0. Let us now focus on deriving the Cutkosky rules for this amplitude. For this we need to compute the difference between (3.1) and (3.2) in the limit $p^0 \to E$ from the first quadrant. Eq. (3.3) shows that in this limit all the poles approach the real axis. The original contour needs to be deformed when Q_4 crosses the imaginary axis so that the poles Q_2 and Q_4 will continue to lie to the left of the integration contour and the poles Q_1 and Q_3 will lie to the right of the integration contour. This has been shown in figure 2. If we include the $i\epsilon$ term, then the poles Q_2 and Q_4 get lifted slightly above the real axis, while the poles Q_1 and Q_3 get shifted slightly below the real axis.

Now as long as $p^0 < \sqrt{\vec{\ell}^2 + m^2} + \sqrt{(\vec{p} - \vec{\ell})^2 + m^2}$, Q_4 lies to the left of Q_1 and the contour can be taken to be invariant under complex conjugation as shown in figure 2. As a result C and C^* are identical.[6] Also all external momenta are real so that the integrands in (3.1) and (3.2) become equal. In this case using (3.1) and (3.2) we see that for the range of values of $\vec{\ell}$ satisfying the above inequality, the contributions to $A(-p_1, -p_2, -p_3, -p_4)^*$ and $A(p_1, p_2, p_3, p_4)$ are equal.

Let us now consider the case when Q_4 approaches Q_1. If we use the $i\epsilon$ prescription, Q_4 always lies above the real axis and Q_1 lies below the real axis, and we can continue to choose

[6] A more general statement is that the new contour obtained after complex conjugation can be deformed to the original contour without passing through a pole.

JHEP10(2016)024

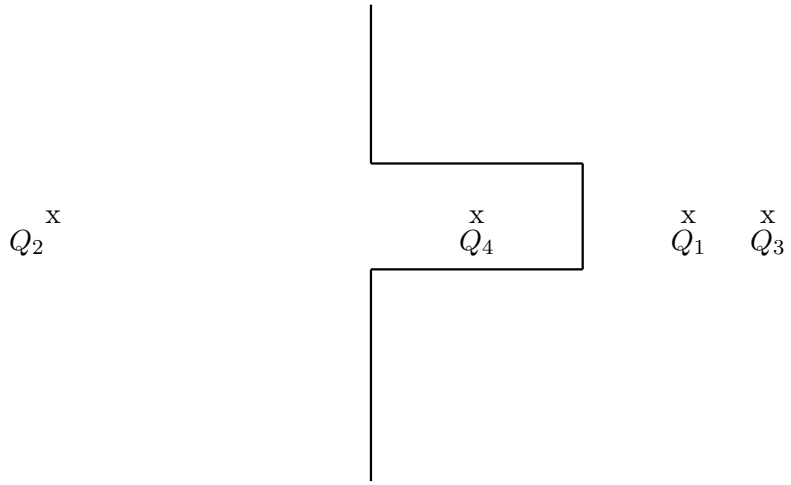

Figure 2. The integration contour over ℓ^0 and the locations of the poles marked by x.

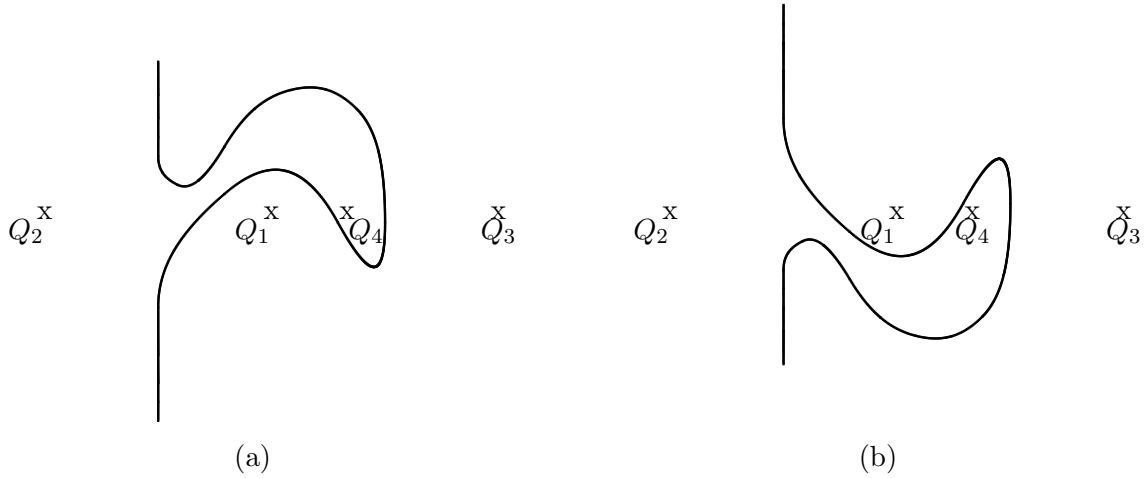

Figure 3. (a) The integration contour over ℓ^0 with the locations of the poles marked by x. (b) The complex conjugate contour.

the contour so that Q_2 and Q_4 are to the left and Q_1 and Q_3 are to the right. However in this case we can no longer ignore the $i\epsilon$ term. Equivalently we can set $\epsilon = 0$ but take p^0 to have a small positive imaginary part as its real part approaches $\sqrt{\vec{\ell}^2 + m^2} + \sqrt{(\vec{p} - \vec{\ell})^2 + m^2}$. In either case, Q_4 lies above Q_1 in the complex plane when their real parts approach each other. We shall return to this contribution later.

For $p^0 > \sqrt{\vec{\ell}^2 + m^2} + \sqrt{(\vec{p} - \vec{\ell})^2 + m^2}$, Q_4 is to the right of Q_1 and the deformed contour takes the form shown in figure 3(a). In drawing this we have used the fact that Q_4 remains above Q_1 as it passes Q_1 and that during this process the contour needs to be deformed continuously without passing through a pole. The complex conjugate contour of figure 3(a) has been shown in figure 3(b). Since in both cases the contours can be taken far away from the poles, we can set the external energies to be real and ϵ to zero so that the integrands in (3.1) and (3.2) become identical. Now even though the contours in figure 3(a) and 3(b) are topologically distinct, each of them can be split into two contours — an anti-

JHEP10(2016)024

clockwise contour around Q_4 and a contour from $-i\infty$ to $i\infty$ keeping Q_1, Q_3 and Q_4 to the right. Therefore their contributions are equal. This shows that integration over the contours in figure 3(a) and figure 3(b) give the same result, and hence the contribution to $A(p_1,p_2,p_3,p_4) - A(-p_1,-p_2,-p_3,-p_4)^*$ from the region of integration where $\vec{\ell}$ satisfies the above inequality also vanishes.

Therefore we see that the contribution to the imaginary part of (3.1) comes from the region around $p^0 \simeq \sqrt{\vec{\ell}^2+m^2} + \sqrt{(\vec{p}-\vec{\ell})^2+m^2}$ when the poles Q_4 and Q_1 approach each other. We shall now evaluate this contribution. For both C and C^*, we proceed by deforming the ℓ^0 contour through the pole Q_4 so that the poles Q_4, Q_1 and Q_3 now lie to the right of the integration contour. This new contour is far away from all poles and can be chosen to be invariant under complex conjugation followed by a reversal of orientation. As a result the integral along this contour gives equal contribution to $A(p_1,p_2,p_3,p_4)$ and $A(-p_1,-p_2,-p_3,-p_4)^*$ according to our previous argument. In the process of passing the contour through Q_4 we also pick up the residue from Q_4. Let us denote by A_r the contribution from the residue at Q_4. This can be expressed as

$$\begin{aligned} A_r = & \int \frac{d^d\ell}{(2\pi)^d} \left\{2\sqrt{(\vec{p}-\vec{\ell})^2+m^2}\right\}^{-1} \\ & \times \left\{p^0 - \sqrt{(\vec{p}-\vec{\ell})^2+m^2} - \sqrt{\vec{\ell}^2+m^2}\right\}^{-1} \left\{p^0 - \sqrt{(\vec{p}-\vec{\ell})^2+m^2} + \sqrt{\vec{\ell}^2+m^2}\right\}^{-1} \\ & \times V^{(4)}(p_1,p_2,-\ell,\ell-p)\, V^{(4)}(\ell,p-\ell,p_3,p_4)\,, \end{aligned} \tag{3.5}$$

where it is understood that ℓ^0 in the argument of $V^{(4)}$ is given by its pole value $p^0 - \sqrt{(\vec{p}-\vec{\ell})^2+m^2}$ and that this contribution is being evaluated only for those values of $\vec{\ell}$ for which p^0 is close to $\sqrt{(\vec{p}-\vec{\ell})^2+m^2} + \sqrt{\vec{\ell}^2+m^2}$ so that Q_4 is close to Q_1. In this case the second term in the second line remains finite over the entire range of integration of $\vec{\ell}$. However the first term in the second line can encounter a divergence. To regulate this we either replace m^2 by $m^2 - i\epsilon$ or take p^0 in the first quadrant. On the other hand for the hermitian conjugate amplitude (3.2) the situation is opposite and we have to either replace m^2 by $m^2 + i\epsilon$ or take $(p^0)^*$ in the fourth quadrant. Using the result

$$(x+i\epsilon)^{-1} - (x-i\epsilon)^{-1} = -2i\pi\delta(x)\,, \tag{3.6}$$

we see that the contribution to $A(p_1,p_2,p_3,p_4) - A(-p_1,-p_2,-p_3,-p_4)^*$ is given by

$$\begin{aligned} & -2\pi\, i \int \frac{d^d\ell}{(2\pi)^d}\, \delta\left(E - \sqrt{(\vec{p}-\vec{\ell})^2+m^2} - \sqrt{\vec{\ell}^2+m^2}\right) \left\{2\sqrt{(\vec{p}-\vec{\ell})^2+m^2}\right\}^{-1} \\ & \quad \times \left\{2\sqrt{\vec{\ell}^2+m^2}\right\}^{-1} V^{(4)}(p_1,p_2,-\ell,\ell-p)\, V^{(4)}(\ell,p-\ell,p_3,p_4)\,, \end{aligned} \tag{3.7}$$

where now all external momenta are taken to be real. Interpreting $V^{(4)}(p_1,p_2,-\ell,\ell-p)$ as the matrix element of T with initial state carrying momentum (p_1,p_2) and final state carrying momentum $(\ell,p-\ell)$ and $V^{(4)}(\ell,p-\ell,p_3,p_4) = V^{(4)}(-\ell,\ell-p,-p_3,-p_4)^*$ as the

JHEP10(2016)024

matrix element of $T^\dagger$ with the initial state carrying momentum $(\ell, p-\ell)$ and the final state carrying momentum $(-p_3, -p_4)$ we see that (3.7) is precisely the statement of the relation

$$T - T^\dagger = -i\, T^\dagger T\,. \tag{3.8}$$

In order to check the precise normalization we must also put back the momentum conserving δ-functions in the expressions for T and $T^\dagger$.

4 Analytic property of general Green's functions

In this section we shall prove the analyticity of the general off-shell Green's function in the first quadrant of the complex λ plane as stated in section 2. More specifically, we shall show that if we restrict the external momenta so that the spatial components are real, and the time components have the form λ times real numbers for a complex parameter λ, then the amplitudes, defined via analytic continuation from imaginary λ axis, are free from any singularities for $\mathrm{Re}(\lambda) \geq 0$, $\mathrm{Im}(\lambda) > 0$. We shall also describe explicitly the procedure for choosing the integration contour that implements the analytic continuation.

4.1 Analyticity in the first quadrant

Our strategy for proving analyticity of the Green's function in the first quadrant of the complex λ-plane will be as follows. We shall show that for any fixed real values of the spatial components $\{\vec{\ell}_k\}$ of the loop momenta, the integral over the $\{\ell_k^0\}$'s can always be deformed away from all singularities of the integrand, i.e. the integration contour is not pinched. As a result the contribution to the integral over $\{\ell_k^0\}$ is non-singular. Since this is true at every $\{\vec{\ell}_k\}$, the result remains non-singular even after integration over $\{\vec{\ell}_k\}$.

We shall prove the result by assuming the contrary and then showing that there is a contradiction. Therefore let us suppose that there is a subspace R of the space spanned by $\{\vec{\ell}_k\}$ where there is a pinch singularity. This means that on this subspace the integrand becomes singular at some points on the ℓ_k^0 integration contours, and we cannot deform the ℓ_k^0 contours away from these points without passing through a singularity. We can classify the regions R of this type using 'reduced diagram' which is obtained from the original Feynman diagram by collapsing all propagators whose energies can be deformed away from the poles. This means that we remove each of these propagators and join the pair of vertices that were originally connected by the propagator into a single vertex with larger number of external legs. The vertices of the reduced diagram will be called reduced vertices. A given reduced vertex may receive contribution from many different Feynman diagrams. We shall assume that the loop energies flowing through the propagators inside the reduced vertex — i.e. the propagators which have been collapsed to points — have been deformed if needed to keep these propagators finite distance away from their poles. Henceforth the propagators of a reduced diagram will refer to only those propagators which have not been collapsed to points.

Let us take any reduced vertex X of the reduced diagram and label by $k_1, \cdots k_s$ the momenta carried away by internal propagators emerging from the vertex. This has been shown in figure 4 with X marking a particular reduced vertex, and A denoting a blob containing arbitrary number of internal lines and reduced vertices. Since each of the internal

JHEP10(2016)024

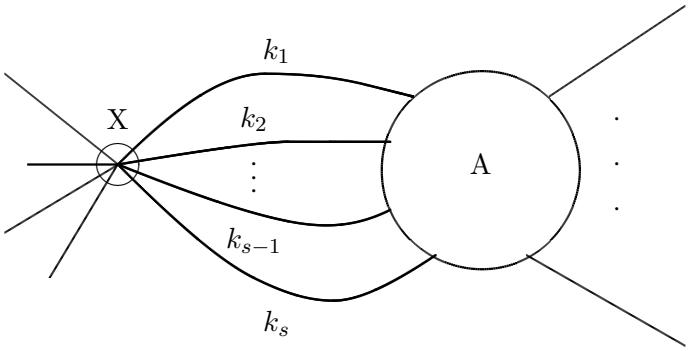

Figure 4. The reduced diagram displaying only the on-shell propagators of a potentially singular region of integration. A denotes a blob containing arbitrary number of internal lines and reduced vertices, and X denotes a specific reduced vertex of this reduced diagram where some external lines are connected.

propagators of the reduced diagram is on-shell at the pinch (otherwise they would have been collapsed to points in the reduced diagram) we have

$$(k_i^0) = \pm\sqrt{\vec{k}_i^2 + m^2} \quad \text{for } 1 \leq i \leq s\,. \tag{4.1}$$

On the other hand if p denotes the total momentum entering the vertex X from the external lines, we have, by momentum conservation,

$$p^0 = \sum_{i=1}^{s} k_i^0\,. \tag{4.2}$$

Now (4.1) shows that k_i^0 is real. Therefore it follows from (4.2) that p^0 must be real. On the other hand we have taken p^0 to be of the form λE for some real number E, with λ lying in the first quadrant. This shows that the only way to satisfy (4.1) and (4.2) for finite $\mathrm{Im}(\lambda)$ is to take $E = 0$. Repeating this analysis for every reduced vertex we see that the total energy entering externally into every reduced vertex of the reduced diagram must vanish.

Let us now denote by the set $\{k_\alpha\}$ the momenta carried by all the propagators of the reduced diagram — not only the ones that leave a given reduced vertex X. Using the $i\epsilon$ convention to label the side of the contour on which a pole lies, we see that the relevant poles at the pinched singularity are at

$$k_\alpha^0 = \pm\sqrt{\vec{k}_\alpha^2 + m^2 - i\epsilon}\,. \tag{4.3}$$

Near the singularities (4.3), we now deform all the loop energy integration contours of the reduced diagram by multiplying them by $\widetilde{\lambda}$ where $\widetilde{\lambda}$ is a complex number close to 1, lying in the first quadrant. Since the deformation is small, it does not lead to any new singularity from the propagators that are inside the reduced vertices. On the other hand since the external energies entering each reduced vertex vanishes, it multiplies each k_α^0 by $\widetilde{\lambda}$. It is easy to see that this deforms the contours away from each of the poles given in (4.3). Therefore the loop energy integration contours are not pinched at the poles (4.3), showing that our initial assumption was incorrect.

This proves the desired result.

JHEP10(2016)024

4.2 Choice of integration contour

For future use, we shall now describe a specific operational procedure for choosing the integration contour. As before we denote by $\{p_i\}$ the external momenta, by $\{\ell_k\}$ the loop momenta and by $\{k_i\}$ the momenta carried by the propagators. We express the n_p propagator factors $(-k_i^2 - m^2)^{-1}$ as $\left(k_i^0 + \sqrt{\vec{k}_i^2 + m^2}\right)^{-1}\left(k_i^0 - \sqrt{\vec{k}_i^2 + m^2}\right)^{-1}$ and assign fixed labels $1, \cdots 2n_p$ to the $2n_p$ poles obtained from the n_p propagators. Our analytic continuation involves choosing the external energies $\{p_i^0\}$ to be $\{\lambda E_i\}$ with real $\{E_i\}$. When λ is on the imaginary axis, each of the ℓ_k^0 integration contours can be taken to run along the imaginary axis from $-i\infty$ to $i\infty$. Furthermore, for each ℓ_k^0 integration contour, there is a definite notion of whether a given pole that depends of ℓ_k^0 lies to the left or right of the integration contour. We make these into permanent assignments in what follows below. As mentioned in section 2 we could keep track of this information using the $i\epsilon$ prescription even when the contours are deformed.

Consider now a general value of λ in the first quadrant, and choose a specific order in which we carry out the integration over $\{\ell_k^0\}$, for fixed values of the spatial components of all loop momenta. Without any loss of generality we can take this order to be $\ell_1^0, \ell_2^0, \ell_3^0, \cdots$. Now let us regard the integrand as a general complex function of $\{\ell_k^0\}$, and for fixed complex values of $\ell_2^0, \ell_3^0, \cdots$, carry out the ℓ_1^0 integration along a contour from $-i\infty$ to $i\infty$ that keeps the ℓ_1^0 dependent poles on the same side of the integration contour as the original contour defined for purely imaginary λ. Note that there may be more than one contour satisfying this condition that are not deformable to each other, e.g. as shown in figure 3(a) and (b). However, the result of integration does not depend on the choice of contour. To see this we note that given any two contours satisfying the above condition, one can be deformed to the other by allowing it to pass through the poles and picking up residues, and during any such deformation a given pole will have to be crossed an even number of times in opposite directions since every time a pole is crossed it moves from the right of the contour to the left or vice versa. Therefore all the residues cancel and the result of integration becomes independent of the choice of contour. This gives a function of $\ell_2^0, \ell_3^0, \cdots$. The resulting function can develop new poles as a function of these variables from the ℓ_1^0 integration. For example a pole in the ℓ_k^0 plane can arise when an ℓ_k^0 dependent pole A in ℓ_1^0 plane collides with an ℓ_k^0 independent pole B in the ℓ_1^0 plane from opposite sides of the contour.[7] We assign this new pole in the ℓ_k^0 plane to be on the same side of the ℓ_k^0 contour that the pole A was before ℓ_1^0 integration. We now carry out the integration over ℓ_2^0 along a contour from $-i\infty$ to $i\infty$ keeping all the ℓ_2^0 dependent poles on the 'correct side' of the contour. Repeating the same argument as before, we get a function of $\ell_3^0, \ell_4^0, \cdots$ with definite assignment of which side of the contours in the $\ell_3^0, \ell_4^0, \cdots$ plane a given pole should lie. This way we can successively carry out the integration over all the ℓ_k^0's and get a finite result as a function of λ, the spatial components of the loop momenta, and

[7] To see that this generates a pole in the ℓ_k^0 plane, we note that the singular part of the integrand has the form $(\ell_1^0 \pm \ell_k^0 - R_A)^{-1}(\ell_1^0 - R_B)^{-1}$ for some R_A and R_B that are independent of ℓ_1^0 and ℓ_k^0. We can deform the ℓ_1^0 contour through the pole B picking up the residue. The deformed contour integral has no singularity from A or B, while the residue at B produces a pole in ℓ_k^0 of the form $(\pm\ell_k^0 - R_A + R_B)^{-1}$.

JHEP10(2016)024

the external momenta. The set of rules defined above for constructing the $\{\ell_k^0\}$ integration contours will be collectively denoted by C.

The complex conjugate contour C^* introduced in section 2, needed for computing the matrix elements of $T^\dagger$, is defined as follows. Let us suppose that the original integration over ℓ_s^0 was done along a contour

$$\ell_s^0 = f_s\left(t; \ell_{s+1}^0, \ell_{s+2}^0, \cdots; \{p_i\}, \{\vec{\ell}_k\}\right), \tag{4.4}$$

for some function f_s of a real variable t labelling the contour, the other ℓ_k^0's for $k > s$, all the external momenta $\{p_i\}$ and the spatial components of all the loop momenta $\{\vec{\ell}_k\}$. The set of functions $\{f_s\}$ is what we collectively call the choice of the contour C. Now the contour in terms of the variables $\{(\ell_k^0)^*\}$ will be

$$(\ell_s^0)^* = \left(f_s\big(t; \ell_{s+1}^0, \ell_{s+2}^0, \cdots; \{p_i\}, \{\vec{\ell}_k\}\big)\right)^* \equiv \widetilde{f}_s\left(t; (\ell_{s+1}^0)^*, (\ell_{s+2}^0)^*, \cdots; \{p_i^*\}, \{\vec{\ell}_k\}\right), \tag{4.5}$$

where we have used the fact that the spatial components of loop momenta are always kept real. After renaming the variables $(\ell_k^0)^*$ as ℓ_k^0, the function $\widetilde{f}_s$ defined this way gives the new ℓ_s^0 integration contour. Operationally $\widetilde{f}_s$ is obtained from f_s by replacing all explicit factors of i by $-i$. We shall denote collectively by C^* the information on the integration contours encoded in the functions $\widetilde{f}_1, \widetilde{f}_2, \cdots$.

5 Cutkosky rules

Our next task is to compute the matrix elements of $T - T^\dagger$ and show that the result is given by Cutkosky rules. The matrix element of T is given by the Green's function $A(\{p_i\}$ for on-shell external momenta $\{p_i\}$ and the matrix element of $T^\dagger$ between the same external states is given by $A(\{-p_i\})^*$. As mentioned before, throughout our analysis we shall keep the spatial components of loop momenta real and allow only the 0-components of the loop momenta to be deformed so as to avoid the poles. It was shown in section 2 that in this case the contributions to $A(\{p_i\}$ and $A(\{-p_i\})^*$ are given by similar integrals with the integrands related by the replacement of p_i by p_i^*, and integration contours C and C^* related by complex conjugation. In absence of pinch singularity we can set the external momenta p_i's to be real and the integrands become identical.

Consider now a pinch singularity where the 0-components of N of the loop momenta are constrained. In this case, in order that each of these N loop momenta are pinched, we need at least $N+1$ of the denominator factors to vanish. This means that there will be at least one constraint among the spatial components of these N loop momenta. More generally we can say that pinch singularities will arise in subspaces of codimension ≥ 1 in the space spanned by the spatial components of the loop momenta. We shall call such subspaces pinched subspaces.[8]

[8]Since we shall eventually look for functions with δ-function support on the pinched subspaces, it is more appropriate to consider subspaces of small thickness around the pinched subspaces.

JHEP10(2016)024

We shall now prove the Cutkosky rules in three steps.

1. We shall begin our analysis with connected diagrams. First we shall show that when the spatial components of loop momenta are away from the pinched subspaces, and the spatial components of the external momenta are away from the subspaces on which some single particle intermediate state is on-shell, the result of carrying out integration over the 0-components of all loop momenta gives the same contribution to $A(\{p_i\}$ and $A(\{-p_i\})^*$. Therefore there is no contribution to $A(\{p_i\} - A(\{-p_i\})^*$ from this region.

2. Then we shall show that for connected diagrams, the contribution to $A(\{p_i\}) - A(\{-p_i\})^*$ from the pinched subspaces and/or from on-shell single particle intermediate states is given by the Cutkosky rules.

3. Finally we shall prove the Cutkosky rules for disconnected diagrams.

Throughout this analysis we shall be using the method of induction, i.e. while proving any of these results for an N-loop amplitude, we shall assume that all the results are valid for any $(N-1)$ loop amplitude. Also during this analysis we ignore the effect of mass renormalization. This is discussed separately in section 5.4.

Due to the iterative nature of our proof, and given that the full analysis is somewhat long, some subtle points may be overlooked if we are not careful. We shall give some examples below:

1. Cutkosky rules, as explained in section 1, require that the part of the diagram on the right of the cut is conjugated. Much of our analysis that follows will go through even if we do not take the hermitian conjugate of the amplitude to the right of the cut. For example in the analysis of the class of diagrams considered in section 5.2.3 we do not need to use explicitly the fact that the part of the diagram to the right of the cut needs to be hermitian conjugated. This may give the reader the impression that for this class of diagrams, Cutkosky rules will hold even if we do not take the hermitian conjugate of the amplitude to the right of the cut. We shall now argue that this is not the case. In section 5.2.2 there is a crucial minus sign on the right hand side of the fourth line of eq. (5.12) that is there due to the hermitian conjugation, and without it the analysis following this equation will not hold. Hermitian conjugation of the amplitude to the right of the cut also plays a crucial role in the analysis of disconnected diagrams in section 5.3. Now while applying recursive methods to the diagrams of section 5.2.3 we often end up with lower order diagrams of the type analyzed in section 5.2.2 and section 5.3, and assume that Cutkosky rules hold for these diagrams. For these we must take the hermitian conjugate of the diagram to the right of the cut. As a result even for the diagrams analyzed in section 5.2.3, Cutkosky rules hold only if we take the hermitian conjugate of the diagram to the right of the cut.

JHEP10(2016)024

2. In our analysis we give an iterative proof that for reduced diagrams, Cutkosky rules require us to sum over only those cut diagrams for which the cut does not pass through a reduced vertex. As usual we assume this to be true to a given order and then prove the result to the next order. The reader may feel somewhat uneasy at the lack of a direct proof, and wonder if the iterative proof would have gone through even if we had relaxed the constraint that the cut does not pass through a reduced vertex. However, if we examine the iterative proof carefully we shall find that during the course of iteration we often end up with diagrams where the whole diagram is a single reduced vertex. The result of section 5.1 shows that this has no anti-hermitian part. This would have been in conflict with the Cutkosky rules if the cuts were allowed to pass through the reduced vertex leading to a non-vanishing result for the anti-hermitian part of the amplitude. Therefore we again see that different parts of the analysis are intimately tied together, and relaxing any ansatz made during one part of the analysis also affects the results of all other parts.

5.1 Hermiticity of the connected diagrams in absence of pinch singularity

In this subsection we shall prove that for connected diagrams, $A(\{p_i\})-A(\{-p_i\})^*$ vanishes in the absence of pinch singularities and on-shell single particle intermediate states. We follow the algorithm described at the end of section 4 to define the analytically continued amplitude as a function of λ in the first quadrant and the amplitude at $\lambda = 1$ as the limit from the first quadrant. As long as there is no pinch singularity at $\lambda = 1$, we can systematically choose the integration contours C over $\ell_1^0, \ell_2^0, \cdots$ appearing in $A(\{p_i\})$, and compute the integrals following the procedure described in section 4. The contribution to $A(\{-p_i\})^*$ can be computed by evaluating the same integral over the integration contours C^*. Since the external momenta are real at $\lambda = 1$ the integrands in the expressions for $A(\{p_i\})$ and $A(\{-p_i\})^*$ are identical. Therefore if we can show that the choice of the contours C and C^* are identical, or deformable to each other without passing through a singularity, we would have proved that the integrals are the same. Actually the same arguments as in section 4.2 shows that we need less — all we need to show is that for each s, the choice of contour in the ℓ_s^0 plane encoded in the functions f_s and $\widetilde{f}_s$ introduced in (4.4) and (4.5) have all the poles lying on the same side, i.e. if a given pole lies on the left (right) of the first contour then it must lie on the left (right) of the second contour.[9] This can be proved by considering the special case where $\ell_{s+1}^0, \ell_{s+2}^0, \cdots$ are real since the side of the contour on which a pole in the ℓ_s^0-plane lies is by construction independent of $\ell_{s+1}^0, \ell_{s+2}^0, \cdots$. For real $\ell_{s+1}^0, \ell_{s+2}^0, \cdots$ the poles in the ℓ_s^0-plane are along the real axis, whereas the ℓ_s^0 integration contours in C and C^* are related by a reflection about the real axis together with a change in orientation. Under this operation the different segments of the real axis lie on the same side of the contours in C and C^* independent of how many times the contours cross the real axis, and hence all the poles on the real axis also lie on the same side of the contours in C and C^*. This establishes the desired result, that the contribution to $A(\{p_i\}) - A(\{-p_i\})^*$ vanishes as long as there is no pinch singularity at $\lambda = 1$.

[9] This includes the case where the contours are not necessarily deformable to each other, as in figure 3(a) and (b).

JHEP10(2016)024

There is one exception to the above result, and this occurs when the external momenta are such that some intermediate one particle state goes on-shell. In this case there are Feynman diagrams in which some propagator carrying momentum p, given by some linear combination of external momenta, blows up. In order to compute the contribution to $A(\{p_i\}) - A(\{-p_i\})^*$ from such Feynman diagrams we again work with a general complex λ and define the amplitude by analytic continuation from imaginary λ-axis to $\lambda = 1$ along the first quadrant. As mentioned before, in $A(\{p_i\})$ this is equivalent to replacing m^2 by $m^2 - i\epsilon$ in the propagator. After going through the manipulations described at the end of section 2 we can bring the expression for $A(\{-p_i\})^*$ to an identical form, except that due to the operation of complex conjugation, in this amplitude m^2 is replaced by $m^2+i\epsilon$. Therefore in the difference between $A(\{p_i\})$ and $A(\{-p_i\})^*$, the propagator $((p^0)^2 - \vec{p}^2 - m^2)^{-1}$ will be replaced by

$$\left((p^0)^2-\vec{p}^2-m^2+i\epsilon\right)^{-1} - \left((p^0)^2 - \vec{p}^2 - m^2 - i\epsilon\right)^{-1} = -2\pi i\,\delta\left((p^0)^2 - \vec{p}^2 - m^2\right). \quad (5.1)$$

This shows that in this case we can get a non-vanishing imaginary part of the amplitude even in the absence of pinch singularity. We shall take into account contributions of this type in our analysis below.

5.2 Anti-hermitian part of connected amplitude

We now turn to the second problem, i.e. the computation of the anti-hermitian part of a connected amplitude when the spatial components of the loop momentum integrals lie on — or more precisely around as stated in footnote 8 — a pinched subspace, or the external momenta lie on a subspace on which some intermediate single particle state goes on-shell. In carrying out the analysis we shall again use the notion of reduced diagram in which we collapse to points all lines which are not put on-shell at the pinch singularity of the energy integration contours. In one particle reducible diagrams we also have internal propagators which are not part of any loop and carries momenta given by linear combinations of the external momenta only. For these lines, we collapse to points those lines which are not on-shell for the specific values of the external momenta we work with. On such a reduced diagram we shall draw an arrow on each of the propagators to indicate the direction of energy flow at the pinch singularity.

We shall now show that the reduced diagram defined this way cannot have a directed closed loop — i.e. a closed loop with the property that we can traverse the loop by following the directions of the arrows. Such a diagram has been shown in figure 5. If there is such a loop, then we can find a loop momentum ℓ that appears only in each propagator in the loop, and the direction of ℓ is along the direction of energy flow for each of the propagators. As a result these propagators will carry momenta $K_i + \ell$ where K_i is linear combination of other loop momenta and external momenta, and at the pinch we have

$$K_i^0 + \ell^0 = \sqrt{(\vec{K}_i + \vec{\ell})^2 + m^2 - i\epsilon}\,. \quad (5.2)$$

Note the + sign on the right hand side, reflecting the fact that ℓ is directed along the energy flow. The $-i\epsilon$ is a formal way of stating the fact all the poles are to the right of the

JHEP10(2016)024

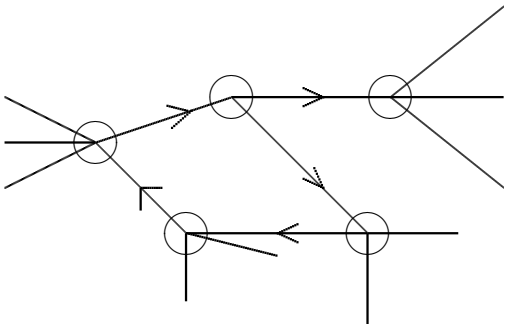

Figure 5. A reduced diagram containing an oriented loop. Such a diagram is not allowed.

ℓ^0 integration contour from $-i\infty$ to $i\infty$. Furthermore there is no other propagator that involves ℓ. It is now easy to see that the ℓ^0 contour is not pinched and can be deformed away keeping all the poles to the right. This proves the desired result.

In what follows, we shall use an even more minimal representation of a reduced diagram in which we suppress all external legs and represent reduced vertices by circles. Furthermore, the absence of an oriented loop in the diagram allows us to do a partial ordering of the vertices in the diagram so that all arrows are directed from the left to the right. With this understanding we can also drop the arrows from the diagram.

5.2.1 Statement of Cutkosky rules for reduced diagrams

Our task will be to compute the contribution to $A(\{p_i\}) - A(\{-p_i\})^*$ from such a reduced diagram and show that the result is consistent with unitarity. For this let us first examine what we need for unitarity. Using $S = 1 - iT$ and the unitarity relation $S^\dagger S = 1$ we get

$$T - T^\dagger = -i\, T^\dagger T\,. \tag{5.3}$$

The computation of $T^\dagger T$ is done by inserting a complete set of states between T and $T^\dagger$. For a multi-particle intermediate state we need to integrate over the spatial components $\vec{k}_i$ of momenta of each particle subject to an overall energy and momentum conserving delta function, and a measure factor

$$\left(2\sqrt{\vec{k}_i^{\,2} + m^2}\right)^{-1}\,. \tag{5.4}$$

We can formally express this as

$$i \int \frac{dk_i^0}{2\pi}\, P_c(k_i)\,, \tag{5.5}$$

where

$$P_c(k_i) \equiv -2\pi i\, \delta\left((k_i^0)^2 - (\vec{k}_i^{\,2} + m^2)\right)\theta(k_i^0)\,, \tag{5.6}$$

and the k_i^0 integral in (5.5) is taken to run along the real axis near the support of the δ-function. The factor (5.6) is precisely what we would get from the residue at the pole of the propagator $((k_i^0)^2 - \vec{k}_i^{\,2} - m^2)^{-1}$ if we take the difference between two contour integrals in the complex k_i^0 plane, one keeping the pole at $k_i^0 = \sqrt{\vec{k}_i^{\,2} + m^2}$ to the right and the other

JHEP10(2016)024

keeping the same pole to the left. We shall denote by a *cut propagator*, with the momentum k flowing from the left to the right of the cut, the effect of replacing a propagator by (5.6). A *cut diagram*, obtained by drawing a line that divides the diagram into a left half and a right half, will involve replacing each cut internal propagator by (5.6) and in addition replacing the amplitude on the right of the cut by its hermitian conjugate. A cut across an external line has no effect. With this convention (5.3) is equivalent to the statement that the amplitude $A(\{p_i\}) - A(\{-p_i\})^*$ will be given by sum over all cut diagrams of the amplitude $A(\{p_i\})$ up to some phases. We shall now describe the origin of these phases and compute them.

1. First of all the $-i$ factor on the right hand side of (5.3) will give an explicit factor of $-i$ multiplying each cut diagram.

2. Replacing each cut propagator by (5.6) will produce the measure factor (5.4) if for each cut propagator there is an integral $idk_i^0/2\pi$ in the original Feynman diagram for $A(\{p_i\})$. If each k_i^0 had represented an independent loop momentum then such a factor will indeed be present according to (2.7). However typically there are energy conserving constraints relating the k_i^0's which reduce the number of k_i^0 integrals, and hence also the number of i's. If there are n_L disconnected components of the diagram to the left of the cut and n_R disconnected components to the right of the cut, then the total number of constraints is $n_L + n_R$. Of these one represents overall energy conservation instead of imposing relations between k_i^0's but the other $n_L + n_R - 1$ constraints reduce the number of independent k_i^0's and hence the number of factors of i. Therefore we need to supply the missing i's by multiplying the cut diagram by a factor of $(i)^{n_L+n_R-1}$ so that we get back the correct number of i's that is needed to get the correct expression for $T^\dagger T$. (The factors of 2π work out automatically since each momentum conserving delta function is accompanied by a factor of 2π.)

3. Eq. (2.6) shows that if the diagram on the left of the cut has n_L disconnected components then the expression for the matrix elements of T should contain an extra factor of $(i)^{-n_L+1}$. Similarly if the diagram on the right of the cut has n_R disconnected components then the matrix element of $T^\dagger$ will contain a net extra factor of $(-i)^{-n_R+1}$ where the replacement of i by $-i$ is due to hermitian conjugation. There is no such factor in the original diagram without cut, since we have assumed that to be connected. Therefore this factor is also absent in the cut diagram, and we need to multiply the cut diagram by a net factor of $(i)^{-n_L+n_R}$.

Combining all these factors we see that we need to weigh a cut diagram by a factor of

$$(-i)(i)^{n_L+n_R-1}(i)^{-n_L+n_R} = (-1)^{n_R-1}\,, \tag{5.7}$$

to reproduce the right hand side of (5.3).

A further simplification of cutting rules is possible for reduced diagrams. Let us consider a cut Feynman diagram in which n propagators carrying momenta $k_1, \cdots k_n$ from left to right are cut. Then we have the relation

$$k_i^0 = \sqrt{\vec{k}_i^2 + m^2}\,. \tag{5.8}$$

Furthermore the k_i's satisfy a momentum conservation law

$$p = \sum_{i=1}^{n} k_i \,, \tag{5.9}$$

where p is some linear combination of external momenta. This imposes constraint on the spatial components $\vec{k}_i$ of the momenta. Now consider the same Feynman diagram without a cut but with the same spatial components of momenta along the propagators that were cut earlier. It is easy to see that the integration contour over k_i^0 for $1 \le i \le (n-1)$ are now pinched at

$$k_i^0 = \sqrt{\vec{k}_i^2 + m^2 - i\epsilon}\,, \qquad p^0 - \sum_{i=1}^{n-1} k_i^0 = \sqrt{(\vec{p} - \vec{k})^2 + m^2 - i\epsilon}\,. \tag{5.10}$$

Reversing this result we see that for fixed spatial momenta flowing along the loops, a Feynman diagram allows a cut passing through propagators $P_1, \cdots P_n$ only if in the original diagram the energy integration contour has a pinch where all the propagators $P_1, \cdots P_n$ are on-shell. This is turn means that in a reduced diagram a cut cannot intersect the propagators inside a reduced vertex. This allows us to state the required Cutkosky rule for a reduced diagram as follows:

> *The contribution to $A(\{p_i\}) - A(\{-p_i\})^*$ from a reduced diagram is given by the sum over all cut diagrams with the cuts avoiding the reduced vertices, weighted by the factor given in* (5.7).

We shall in fact prove a slightly more general result. Consider an amplitude in which we have replaced the integration contour C required to compute $A(\{p_i\})$ by a different contour $\widetilde{C}$ leaving the integrand unchanged. Let us call this contribution $\widetilde{A}(\{p_i\})$. We again work at fixed values of the spatial components of loop momenta, and define R as the original reduced diagram associated with integration along the contour C and $\widetilde{R}$ as the reduced diagram obtained by shrinking to points all propagators which are not pinched in $\widetilde{C}$. We shall show that the version of the Cutkosky rules for reduced diagrams, as stated above, holds for $\widetilde{R}$ as long as the poles coming from the surviving propagators in $\widetilde{R}$ lie on the same side of the integration contour $\widetilde{C}$ as they were for C. However there is no restriction on how the poles associated with the propagators inside the reduced vertices of $\widetilde{R}$ are situated relative to $\widetilde{C}$ as long as there is no pinch singularity that prevents us from deforming $\widetilde{C}$ away from these poles. In particular even if the original contour C was pinched at the poles of some of the propagators inside a reduced vertex of $\widetilde{R}$, Cutkosky rules for $\widetilde{R}$ will not include sum over cuts passing through this reduced vertex.

We shall prove this in two steps.

1. First we shall introduce the notion of one vertex irreducible (1VI) and one vertex reducible (1VR) reduced diagrams and show that the Cutkosky rules for 1VR diagrams hold as long as they hold for 1VI diagrams.

2. Then we shall prove the Cutkosky rules for 1VI reduced diagram.

JHEP10(2016)024

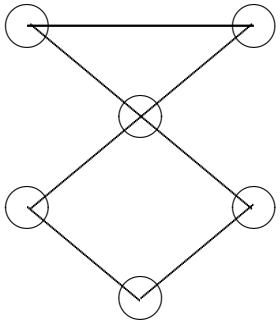

Figure 6. Example of a 1VR diagram. The external lines are suppressed, the reduced vertices are denoted by circles, and the arrows on all lines are understood to be directed towards the right.

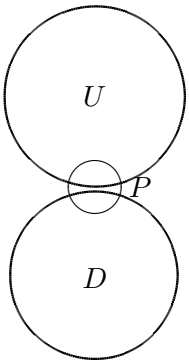

Figure 7. Schematic representation of a 1VR reduced diagram consisting of two components U and D joined at a single reduced vertex P. All external lines have been suppressed.

5.2.2 One vertex reducible reduced diagrams

We shall define a reduced diagram to be 1VR if it can be regarded as two reduced diagrams joined at a single reduced vertex. An example of such a diagram has been shown in figure 6. Reduced diagrams which are not 1VR will be called 1VI. We shall now show that for a 1VR reduced diagram, the Cutkosky rules follow if they hold for the individual components that are joined at a single reduced vertex to produce the 1VR diagram. By repeated application of this result, one can then show that the Cutkosky rules will hold for a general reduced diagram as long as they hold for 1VI diagrams.

Let us consider a 1VR diagram shown in figure 7 consisting of two pieces U and D connected at a single reduced vertex P. U and D may be either 1VI or 1VR — our analysis holds in all cases. In general the contribution from the reduced vertex P will depend on the momenta entering it from the blobs U and D and the amplitude will not be factorized. First let us assume that the dependence on these momenta are factorized so that the full amplitude can be regarded as a product of the amplitudes associated with the two blobs — we shall deal with the general case later. We denote by A_U and A_D the amplitudes associated with the reduced diagrams U and D. Then the full amplitude is given by $A_U A_D$. Our goal will be to show that $A_U A_D - A_U^* A_D^*$ is given by the sum over cut diagrams of the full diagram weighted by the phase factor (5.7), if we assume that similar result holds for

JHEP10(2016)024

$A_U - A_U^*$ and $A_D - A_D^*$. Now since the cuts do not pass through the reduced vertex P, the cut diagrams of A_U and A_D can be divided into two parts, those with the cut on the left of the vertex P and those with the cut on the right of the vertex P. We denote by Δ_{UL}, Δ_{UR}, Δ_{DL} and Δ_{DR} respectively the sum over all cut diagrams, weighted by (5.7), (a) of U with the cut on the left of P, (b) of U with the cut on the right of P, (c) of D with the cut on the left of P and (d) of D with the cut on the right of P. Then the assumption that the diagrams U and D satisfy Cutkosky rules imply that

$$A_U - A_U^* = \Delta_{UL} + \Delta_{UR}, \qquad A_D - A_D^* = \Delta_{DL} + \Delta_{DR}\,. \tag{5.11}$$

We shall now compute the sum over all cut diagrams of the full diagram shown in figure 7. These diagrams can be divided into six classes. Two of them, described by the first two lines of (5.12), are shown in figures 8(a) and (b) respectively; the rest can be drawn in a similar fashion. Below we describe these six classes of cut diagrams and their contribution:

$$\begin{aligned}
\text{cuts of } D \text{ on the left of } P, \text{ passing on the left of } U: &\quad A_U^*\Delta_{DL}\\
\text{cuts of } D \text{ on the left of } P, \text{ cuts of } U \text{ on the left of } P: &\quad \Delta_{UL}\Delta_{DL}\\
\text{cuts of } U \text{ on the left of } P, \text{ passing on the left of } D: &\quad \Delta_{UL}A_D^*\\
\text{cuts of } D \text{ on the right of } P, \text{ cuts of } U \text{ on the right of } P: &\quad -\Delta_{UR}\Delta_{DR}\\
\text{cuts of } D \text{ on the right of } P, \text{ passing on the right of } U: &\quad A_U\Delta_{DR}\\
\text{cuts of } U \text{ on the right of } P, \text{ passing on the right of } D: &\quad \Delta_{UR}A_D\,.
\end{aligned} \tag{5.12}$$

The minus sign on the right hand side of the fourth line is a consequence of (5.7) and the fact that $n_R - 1$ for the corresponding cut is given by $(n_{UR} - 1) + (n_{DR} - 1) + 1$. The sum of these, using (5.11), can be easily seen to be given by

$$A_U A_D - A_U^* A_D^*\,. \tag{5.13}$$

This is precisely the Cutkosky rule for the full diagram. This proves the desired relation.

Let us now turn to the general case where the reduced vertex P depends on the momenta entering it from both U and D, and the contribution is not factorized. Let us denote by $\{\ell_{U,i}\}$ the momenta entering P from U and by $\{\ell_{D,i}\}$ the momenta entering P from D. Each set satisfies an overall momentum conservation constraint that sets $\sum_i \ell_{U,i} = -\sum_i \ell_{D,i}$ to some linear combination of external momenta giving the total momentum flowing across the reduced vertex P. Our starting assumption will be that for fixed $\{\ell_{D,i}\}$ the sub-diagram U, including the contribution from the reduced vertex P, satisfies the Cutkosky rules and that for fixed $\{\ell_{U,i}\}$ the subdiagram D, including the contribution from the reduced vertex P, satisfies the Cutkosky rules. Let us denote the corresponding amplitudes by A_U and A_D respectively, and the sum over cuts as described above (5.11) by Δ_{UR}, Δ_{UL}, Δ_{DR} and Δ_{DL} so that (5.11) holds. We also denote by $V_P(\{\ell_{U,i}\}, \{\ell_{D,i}\})$ the contribution from the reduced vertex P, and by a_U, a_U^*, δ_{UL} and δ_{UR} the quantities appearing in the expressions for A_U, A_U^*, Δ_{UL}, Δ_{UR} introduced above (5.11), *before doing integration over* $\{\ell_{U,i}\}$ *and without including the contribution* V_P *from the reduced vertex.* a_D, a_D^*, δ_{DL} and δ_{DR} will denote similar contributions that would enter the computation

JHEP10(2016)024

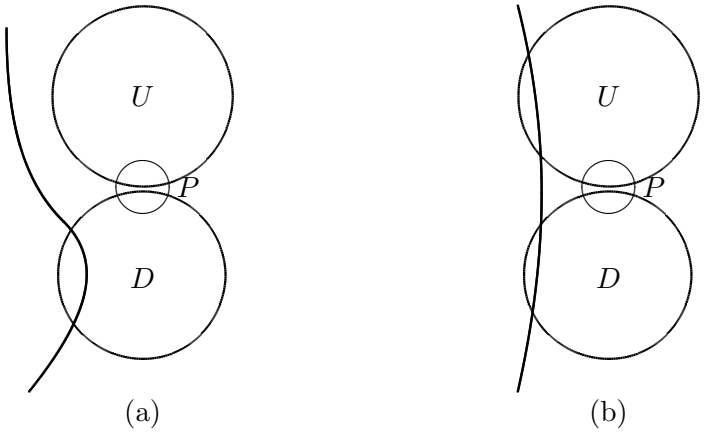

Figure 8. Cut diagrams of the reduced diagram of figure 7 corresponding to the first and the second line of (5.12).

of A_D, A_D^*, Δ_{DL} and Δ_{DR}. In that case a_U, a_U^*, δ_{UL} and δ_{UR} depend on $\{\ell_{U,i}\}$ but not on $\{\ell_{D,i}\}$ and a_D, a_D^*, δ_{DL} and δ_{DR} depend on $\{\ell_{D,i}\}$ but not on $\{\ell_{U,i}\}$. We now have

$$\begin{aligned}
&A_U = \int_{\{\ell^0_{U,i}\}} a_U V_P, \quad A_U^* = \int_{\{\ell^0_{U,i}\}} a_U^* V_P, \quad \Delta_{UL} = \int_{\{\ell^0_{U,i}\}} \delta_{UL} V_P, \quad \Delta_{UR} = \int_{\{\ell^0_{U,i}\}} \delta_{UR} V_P\,, \\
&A_D = \int_{\{\ell^0_{D,i}\}} a_D V_P, \quad A_D^* = \int_{\{\ell^0_{D,i}\}} a_D^* V_P, \quad \Delta_{DL} = \int_{\{\ell^0_{D,i}\}} \delta_{DL} V_P, \quad \Delta_{DR} = \int_{\{\ell^0_{D,i}\}} \delta_{DR} V_P\,.
\end{aligned} \tag{5.14}$$

In these equations it is understood that while doing the integration over $\{\ell^0_{U,i}\}$ and $\{\ell^0_{D,i}\}$, the choice of integration contour may depend on the integrand. For example the integration contours for $\{\ell^0_{U,i}\}$ for integral over a_U and a_U^* may not be the same. Also note that we have not included integration over the spatial components of $\{\ell_{U,i}\}$ and $\{\ell_{D,i}\}$ since we have been working at fixed values of the spatial components of loop momenta. Eq. (5.11) now takes the form

$$\int_{\{\ell^0_{U,i}\}} (a_U - a_U^*) V_P = \int_{\{\ell^0_{U,i}\}} (\delta_{UL} + \delta_{UR}) V_P, \quad \int_{\{\ell^0_{D,i}\}} (a_D - a_D^*) V_P = \int_{\{\ell^0_{D,i}\}} (\delta_{DL} + \delta_{DR}) V_P\,. \tag{5.15}$$

Eq. (5.12) can be similarly generalized, leading to the following contribution to the sum over cut diagrams of figure 7:

$$\int_{\{\ell^0_{U,i}\}} \int_{\{\ell^0_{D,i}\}} \Big(a_U^* \delta_{DL} + \delta_{UL}\delta_{DL} + \delta_{UL} a_D^* - \delta_{UR}\delta_{DR} + a_U \delta_{DR} + \delta_{UR} a_D \Big) V_P\,. \tag{5.16}$$

Again we should keep in mind that for different integrands we have to integrate over different contours. After some algebra using (5.15), the expression (5.16) can be brought to the form

$$\int_{\{\ell^0_{U,i}\}} \int_{\{\ell^0_{D,i}\}} (a_U a_D - a_U^* a_D^*)\, V_P\,. \tag{5.17}$$

This is precisely the difference between the original amplitude shown in figure 7 and its hermitian conjugate. This gives the desired result.

JHEP10(2016)024

5.2.3 One vertex irreducible reduced diagrams

We now turn to the task of proving Cutkosky rules for 1VI diagrams. As mentioned before, we shall carry out the proof recursively, i.e. assume that the result holds for all reduced diagrams with $(N-1)$ loops and then prove that the result holds for 1VI reduced diagrams with N loops. To this end let us consider a 1VI reduced diagram with N loops and label the independent loop momenta by $\ell_1, \cdots \ell_N$. We now consider the particular loop S that carries loop momentum ℓ_1 and analyze the integral over ℓ_1^0 at fixed values of other loop momenta. Let us suppose that as we traverse this loop along the direction of ℓ_1, n of the propagators in the loop — which we denote by $P_1, \cdots P_n$ — have their arrows directed along ℓ_1 while the others have their arrows directed opposite to ℓ_1. In that case near the pinch the relevant pole in the ℓ_1^0 plane from the propagator P_i has the form

$$\left(-(\ell_1+K_i)^2 - m^2 + i\epsilon\right)^{-1} \theta(\ell_1^0 + K_i^0)\,, \tag{5.18}$$

for $1 \le i \le n$. Here K_i's are linear combinations of the external momenta and other loop momenta in the reduced diagram. The $\theta(\ell_1^0 + K_i^0)$ is a formal expression that tells us that at the pinch the relevant pole is the one that appears at positive value of $\ell_1^0 + K_i^0$. The $i\epsilon$ prescription reflects that for the ℓ_1^0 integration contour beginning at $-i\infty$ and ending at $i\infty$, the pole of (5.18) lies to the right of the integration contour. On the other hand the poles from all other propagators in the loop S that are not in the set $P_1, \cdots P_n$ lie to the left of the ℓ_1^0 integration contour. We denote by C the original integration contour, and by C^* the integration contour needed to compute the hermitian conjugate amplitude. Below we follow the convention that for any contour $\mathcal{C}$ required for computing an amplitude, $\mathcal{C}^*$ will denote the integration contour required to compute the hermitian conjugate of the amplitude.

We shall now deform the integration contours of ℓ_1^0 in C through each of the poles given in (5.18) to the other side, at the expense of picking up residues at the poles. Let us denote the deformed integration contour by $\widehat{C}$ and the amplitude obtained by integrating over this deformed contour by $\widehat{A}$. This contour will have all the relevant poles in the ℓ_1^0 plane to the left of the integration contour and hence the contour is not pinched. Therefore by deforming the ℓ_1^0 integration contours we can ensure that the momenta along all the propagators in the loop S can be deformed away from the on-shell values. On the other hand the difference between the original amplitude A and the new amplitude $\widehat{A}$ is given by the sum of residues at the poles (5.18) through which we deform the contour. This may be computed using the relation

$$\begin{aligned}
&\prod_{i=1}^n \left\{\left(-(\ell_1+K_i)^2 - m^2 - i\epsilon\right)^{-1} \theta(\ell_1^0 + K_i^0)\right\} \qquad (5.19)\\
&= \prod_{i=1}^n \left\{\left(-(\ell_1+K_i)^2 - m^2 + i\epsilon\right)^{-1} \theta(\ell_1^0 + K_i^0) + 2\pi i\,\delta\left((\ell_1+K_i)^2 + m^2\right)\theta(\ell_1^0 + K_i^0)\right\}\,,
\end{aligned}$$

which gives

$$
\begin{aligned}
&\prod_{i=1}^{n}\left(-(\ell_1+K_i)^2-m^2+i\epsilon\right)^{-1}\theta(\ell_1^0+K_i^0)\\
&=\prod_{i=1}^{n}\left(-(\ell_1+K_i)^2-m^2-i\epsilon\right)^{-1}\theta(\ell_1^0+K_i^0)\\
&\quad+\sum_{j=1}^{n}\left\{-2\pi i\,\delta\left((\ell_1+K_j)^2+m^2\right)\theta(\ell_1^0+K_j^0)\right\}\prod_{\substack{i=1\\ i\neq j}}^{n}\left(-(\ell_1+K_i)^2-m^2+i\epsilon\right)^{-1}\theta(\ell_1^0+K_i^0)\\
&\quad-\sum_{\substack{j,k=1\\ j<k}}^{n}\left\{-2\pi i\,\delta\left((\ell_1+K_j)^2+m^2\right)\theta(\ell_1^0+K_j^0)\right\}\left\{-2\pi i\,\delta\left((\ell_1+K_k)^2+m^2\right)\theta(\ell_1^0+K_k^0)\right\}\\
&\qquad\times\prod_{\substack{i=1\\ i\neq j,k}}^{n}\left(-(\ell_1+K_i)^2-m^2+i\epsilon\right)^{-1}\theta(\ell_1^0+K_i^0)\\
&\quad+\cdots\\
&\quad+(-1)^{n-1}\prod_{j=1}^{n}\left\{-2\pi i\,\delta\left((\ell_1+K_j)^2+m^2\right)\theta(\ell_1^0+K_j^0)\right\}.
\end{aligned}
\tag{5.20}
$$

The $(-2\pi i)\,\delta\left((\ell_1+K_j)^2+m^2\right)\theta(\ell_1^0+K_j^0)$ factor should again be regarded as a formal expression that has to be made sense of by regarding the $\ell_1^0+K_j^0$ integration to be along the real axis near the pinch singularity. The product over the propagator factors given in the left hand side of (5.20) appears in the integrand needed for computing the amplitude A. When we replace this by the right hand side of (5.20) inside the integral, the first term on the right hand side represents integration over the deformed contour $\widehat{C}$ generating the amplitude $\widehat{A}$ and the other terms on the right hand side represent the residues at various poles from the propagators $P_1,\cdots P_n$ picked up during the deformation from C to $\widehat{C}$. Comparison with the right hand side of (5.6) shows that the effect of replacing the propagator P_j by the $(-2\pi i)\delta\left((\ell_1+K_j)^2+m^2\right)\theta(\ell_1^0+K_j^0)$ factor may be represented by a cut on the j-th propagator. Let us denote by $A^{(j)}$ the amplitude obtained by replacing the propagator P_j by the cut propagator in the original amplitude. More generally we denote by $A^{(i_1\cdots i_s)}$ the amplitude obtained by replacing the propagators $P_{i_1},\cdots P_{i_s}$ by cut propagators. Then (5.20) inside the integral translates to

$$
A=\widehat{A}+\sum_{j=1}^{n}A^{(j)}-\sum_{\substack{j,k=1\\ j<k}}^{n}A^{(jk)}+\cdots+(-1)^{n-1}A^{(12\cdots n)}\,.
\tag{5.21}
$$

Even though $A^{(i_1\cdots i_s)}$ is obtained from the original amplitude A by replacing some of its internal propagators by cut propagators, it is important to recognize that $A^{(i_1\cdots i_s)}$ is not a cut diagram. There is no cut separating the graph into two parts and there is no part of the diagram that is to be replaced by its hermitian conjugate. Therefore it is more appropriate to interpret $A^{(i_1\cdots i_s)}$ as an amplitude where the propagators $P_{i_1},\cdots P_{i_s}$ have been replaced by on-shell external states. Furthermore, since all the propagators factors on

JHEP10(2016)024

the right hand side of (5.20) except the first term have the correct $i\epsilon$ prescription, $A^{(i_1\cdots i_s)}$ is defined in the same way as the original amplitude A, i.e. by taking all the external state energies to be λE_s for real E_s, and then taking the $\lambda \to 1$ limit from the first quadrant.

We can also carry out a similar manipulation for the hermitian conjugate amplitude A^*.[10] Manipulations similar to the one given above, applied to A^*, give

$$A^* = \widehat{A}^* + \sum_{j=1}^{n} A^{(j)*} - \sum_{\substack{j,k=1\\ j<k}}^{n} A^{(jk)*} + \cdots + (-1)^{n-1} A^{(12\cdots n)*} \,. \tag{5.22}$$

Since $A^{(i_1\cdots i_s)}$ has less number of loops than the original diagram contributing to the amplitude A, the Cutkosky rules hold for $A^{(i_1\cdots i_s)}$. Therefore the anti-hermitian part of $A^{(i_1\cdots i_s)}$ is given by the sum over all its cut diagrams. We denote by $A^{(i_1\cdots i_s)}_{j_1\cdots j_r}$ the sum over all cut diagrams of the amplitude $A^{(i_1\cdots i_s)}$, for which the cut passes through $P_{j_1}, \cdots P_{j_r}$ and possibly other propagators, but not any of the other P_i's in the set $\{P_1, \cdots P_n\}$. Some examples of this have been shown in figure 9. $A^{(i_1\cdots i_s)}_{\emptyset}$ will denote the sum over all the cut diagrams of $A^{(i_1\cdots i_s)}$ for which the cut does not pass through any of the propagators in the set $\{P_1, \cdots P_n\}$. Then we may express the Cutkosky rule applied to the amplitude associated with $A^{(i_1\cdots i_s)}$ as

$$A^{(i_1\cdots i_s)} - A^{(i_1\cdots i_s)*} = A^{(i_1\cdots i_s)}_{\emptyset} + \sum_{j_1=1}^{n} A^{(i_1\cdots i_s)}_{j_1} + \sum_{\substack{j_1,j_2=1\\ j_1<j_2}}^{n} A^{(i_1\cdots i_s)}_{j_1 j_2} + \cdots + A^{(i_1\cdots i_s)}_{1\cdots n} \,. \tag{5.23}$$

By construction the right hand side of this equation exhausts all cut diagrams of the amplitude $A^{(i_1\cdots i_s)}$. Using this and (5.21), (5.22) we get

$$\begin{aligned} A - A^* = \widehat{A} - \widehat{A}^* &+ \sum_{i=1}^{n} \left[A^{(i)}_{\emptyset} + \sum_{j_1=1}^{n} A^{(i)}_{j_1} + \sum_{\substack{j_1,j_2=1\\ j_1<j_2}}^{n} A^{(i)}_{j_1 j_2} + \cdots + A^{(i)}_{1\cdots n} \right] \\ &- \sum_{\substack{i,j=1\\ i<j}}^{n} \left[A^{(ij)}_{\emptyset} + \sum_{j_1=1}^{n} A^{(ij)}_{j_1} + \sum_{\substack{j_1,j_2=1\\ j_1<j_2}}^{n} A^{(ij)}_{j_1 j_2} + \cdots + A^{(ij)}_{1\cdots n} \right] \\ &+ \cdots \\ &+ (-1)^{n-1} \left[A^{(12\cdots n)}_{\emptyset} + \sum_{j_1=1}^{n} A^{(12\cdots n)}_{j_1} + \sum_{\substack{j_1,j_2=1\\ j_1<j_2}}^{n} A^{(12\cdots n)}_{j_1 j_2} + \cdots + A^{(12\cdots n)}_{1\cdots n} \right] . \end{aligned} \tag{5.24}$$

We now note the following relations. First of all, since we have seen that in $\widehat{A}$ the ℓ_1^0 contour is not pinched, the loop S can be shrunk to a reduced vertex. The resulting

[10] Naively one might expect that the effect of hermitian conjugation will change the i's to $-i$ in the expression for the cut propagators, and hence give an extra minus sign for each cut propagator. However the way we have defined the contour C^* involves a complex conjugation together with orientation reversal, and this ensures that any given pole lies on the same side of C and C^*. Therefore during the deformation from C to $\widehat{C}$ and C^* to $\widehat{C}^*$ we cross various poles in the same direction, and there is no minus sign in the expression for the cut propagators of the hermitian conjugate amplitude A^*.

JHEP10(2016)024

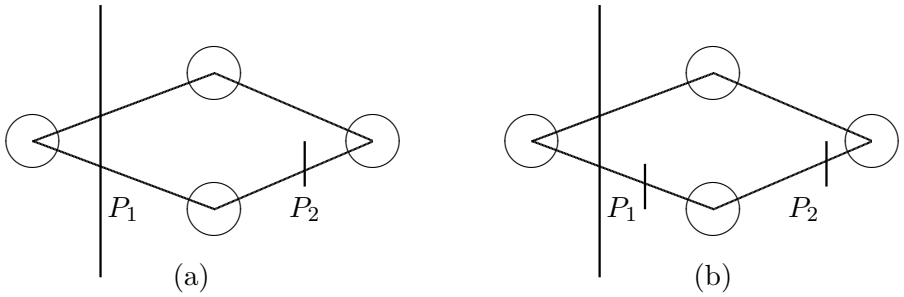

Figure 9. Figure (a) shows a cut reduced diagram in which a propagator P_2 is replaced by a cut propagator in the original diagram and the cut passes through the propagator P_1. In our notation this will be labelled as $A_1^{(2)}$. Figure (b) shows a cut reduced diagram in which propagators P_1 and P_2 are replaced by cut propagators in the original diagram and the cut passes through the propagator P_1. In our notation this will be labelled as $A_1^{(12)}$. These two contributions are identical. In this example there is no cut diagram in which the cut passes through both the propagators P_1 and P_2, and hence $A_{12}^{(12)} = 0$. But this is not always the case.

reduced diagram has one less loop than the original diagram, and hence the Cutkosky rules should hold for this diagram. Furthermore in none of the cut diagrams of this diagram the cut will pass through any of the propagators P_i since they have all been shrunk to a reduced vertex. This gives, in our previous notation,[11]

$$\widehat{A} - \widehat{A}^* = \widehat{A}_\emptyset \,. \tag{5.25}$$

Second we note that in $A_{j_1\cdots j_r}^{(i_1\cdots i_s)}$ the cut passes through the propagators $P_{j_1}, \cdots P_{j_r}$ putting them on-shell, and the propagators $P_{i_1}, \cdots P_{i_s}$ are replaced by cut propagators, putting them on-shell from the beginning. Therefore the result remains the same if we append to the set $i_1, \cdots i_s$ appearing in the superscript one or more elements of the set $\{j_1, \cdots j_r\}$ that are not already part of $\{i_1, \cdots i_s\}$. This has been illustrated in figure 9. This gives

$$A_{j_1\cdots j_r}^{(i_1\cdots i_s)} = A_{j_1\cdots j_r}^{(\{i_1,\cdots i_s\}\cup\{j_1,\cdots j_r\})} \,. \tag{5.26}$$

Using this we can compute the coefficient of $A_{j_1\cdots j_r}^{(i_1\cdots i_s)}$ on the right hand side of (5.24) as follows. Due to (5.26) we can choose the independent A's to be of the form $A_{j_1\cdots j_r}^{(i_1\cdots i_s j_1\cdots j_r)}$ with $\{i_1, \cdots i_s\} \cap \{j_1, \cdots j_r\} = \emptyset$. In this case for $s \neq 0$, $r \neq 0$, the coefficient of $A_{j_1\cdots j_r}^{(i_1\cdots i_s j_1\cdots j_r)}$ comes from the following terms in (5.24):

$$\begin{aligned}
A_{j_1\cdots j_r}^{(i_1\cdots i_s)} &: (-1)^{s-1} \\
A_{j_1\cdots j_r}^{(i_1\cdots i_s j_m)} &: (-1)^{s} \qquad \text{for } 1 \le m \le r \\
A_{j_1\cdots j_r}^{(i_1\cdots i_s j_m j_p)} &: (-1)^{s+1} \qquad \text{for } 1 \le m < p \le r \\
\cdots &: \cdots \\
A_{j_1\cdots j_r}^{(i_1\cdots i_s j_1\cdots j_r)} &: (-1)^{s+r-1}
\end{aligned} \tag{5.27}$$

[11] Note that (5.25) requires the generalization of the Cutkosky rules for the reduced diagrams mentioned at the end of section 5.2.1.

JHEP10(2016)024

The net contribution to the coefficient from all the terms is given by

$$(-1)^{s-1}\left[1-r+\binom{r}{2}-\cdots+(-1)^r\binom{r}{r}\right]=(-1)^{s-1}(1-1)^r=0\,. \tag{5.28}$$

For $s=0$, i.e. for $A^{(j_1\cdots j_r)}_{j_1\cdots j_r}$, the first line of (5.27) will be missing. As a result the contribution is given by

$$-\left[-r+\binom{r}{2}-\cdots+(-1)^r\binom{r}{r}\right]=1-(1-1)^r=1\,. \tag{5.29}$$

Finally for $r=0$, i.e. for $A^{(i_1\cdots i_s)}_{\emptyset}$, only the term in the first line of (5.27) is present and the contribution is given by

$$(-1)^{s-1}\,. \tag{5.30}$$

This, together with (5.25) can be used to rewrite (5.24) as

$$\begin{aligned}A-A^* = \widehat{A}_\emptyset &+\sum_{i=1}^n A^{(i)}_i+\sum_{\substack{i,j=1\\ i<j}}^n A^{(ij)}_{ij}+\cdots+A^{(1\cdots n)}_{1\cdots n}\\ &+\sum_{i=1}^n A^{(i)}_\emptyset-\sum_{\substack{i,j=1\\ i<j}}^n A^{(ij)}_\emptyset+\cdots+(-1)^{n-1}A^{(1\cdots n)}_\emptyset\,.\end{aligned} \tag{5.31}$$

In order to show that the Cutkosky rules hold for the amplitude associated with A, we have to show that the right hand side of (5.31) agrees with the sum of all the cut diagrams of this amplitude. Let us denote by $A_\emptyset$ the sum of cut diagrams of A in which the cut does not pass through any of the propagator $P_1,\cdots P_n$, and by $A_{i_1\cdots i_s}$ the sum of cut diagrams of A in which the cut passes through the propagators $P_{i_1},\cdots P_{i_s}$ and possibly other propagators but not any of the other propagators in the set $\{P_1,\cdots P_n\}$. Then the sum over all the cut diagrams of A is given by

$$A_\emptyset+\sum_{i=1}^n A_i+\sum_{1\le i<j\le n} A_{ij}+\cdots+A_{1\cdots n}\,. \tag{5.32}$$

Since in $A_{i_1\cdots i_s}$ the propagators $P_{i_1},\cdots P_{i_s}$ are put on-shell, we have

$$A_{i_1\cdots i_s}=A^{(i_1\cdots i_s)}_{i_1\cdots i_s}\,. \tag{5.33}$$

On the other hand since in $A_\emptyset$ none of the propagators $P_1,\cdots P_n$ are cut, the cut does not enter the loop S. As a result the entire loop lies on one side of the cut. We can now repeat the analysis that led to (5.21), (5.22) on the sub-diagram of $A_\emptyset$ that contains the loop S, leading to

$$A_\emptyset=\widehat{A}_\emptyset+\sum_{i=1}^n A^{(i)}_\emptyset-\sum_{\substack{i,j=1\\ i<j}}^n A^{(ij)}_\emptyset+\cdots+(-1)^{n-1}A^{(12\cdots n)}_\emptyset\,. \tag{5.34}$$

JHEP10(2016)024

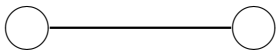

Figure 10. A reduced diagram containing a single propagator.

Substituting (5.33) and (5.34) into (5.32) we get the following expression for the sum over all the cut diagrams of A:

$$\begin{aligned}&\widehat{A}_\emptyset + \sum_{i=1}^n A_\emptyset^{(i)} - \sum_{\substack{i,j=1\\ i<j}}^n A_\emptyset^{(ij)} + \cdots + (-1)^{n-1} A_\emptyset^{(1\cdots n)} \\ &+ \sum_{i=1}^n A_i^{(i)} + \sum_{\substack{i,j=1\\ i<j}}^n A_{ij}^{(ij)} + \cdots + A_{1\cdots n}^{(1\cdots n)} \,. \end{aligned} \tag{5.35}$$

This precisely agrees with the right hand side of (5.31). This shows that the Cutkosky rules hold for the 1VI reduced diagrams with N loops if it holds for amplitudes with $\leq (N-1)$ loops.

In order to complete the proof we need to verify that the result holds for 1VI reduced diagrams with zero loops. This corresponds to two reduced vertices connected by a single propagator as shown in figure 10. If p denotes the momentum flowing from the left to the right then p^0 is positive by convention, and the contribution to the diagram is given by

$$A(p) = \frac{1}{(p^0)^2 - \vec{p}^{\,2} - m^2 + i\epsilon} F(p) \,, \tag{5.36}$$

where $F(p)$ is the contribution from the reduced vertices. The $i\epsilon$ factor is equivalent to defining this amplitude via analytic continuation of the amplitude with p^0 replaced by λp^0, and taking the limit $\lambda \to 1$ from the first quadrant of the complex λ-plane. Now since the reduced vertices are not pinched we have $F(p)^* = F(-p)$ for real p and hence

$$\begin{aligned} A(p) - A(-p)^* &= \left[\frac{1}{(p^0)^2 - \vec{p}^{\,2} - m^2 + i\epsilon} - \frac{1}{(p^0)^2 - \vec{p}^{\,2} - m^2 - i\epsilon} \right] F(p) \\ &= -2\pi i\, \delta\left((p^0)^2 - \vec{p}^{\,2} - m^2\right) \theta(p^0) F(p) \,, \end{aligned} \tag{5.37}$$

where the $\theta(p^0)$ factor has been included since we are considering positive p^0 anyway. Comparison with (5.6) shows that this precisely corresponds to replacing the propagator in figure 10 by the cut propagator, in accordance with the Cutkosky rules.

5.3 Amplitudes with disconnected components

Finally we turn to the proof of Cutkosky rules for amplitudes with disconnected components. We shall prove the result by showing that if an amplitude has two disconnected components A and B, each of which may be connected or disconnected, then as long as the Cutkosky rules hold for A and B, they also hold for the diagram with components A and B. Repeated use of this result, and the fact that Cutkosky rules hold for connected diagrams, then proves that Cutkosky rules hold for diagrams with arbitrary number of disconnected components.

JHEP10(2016)024

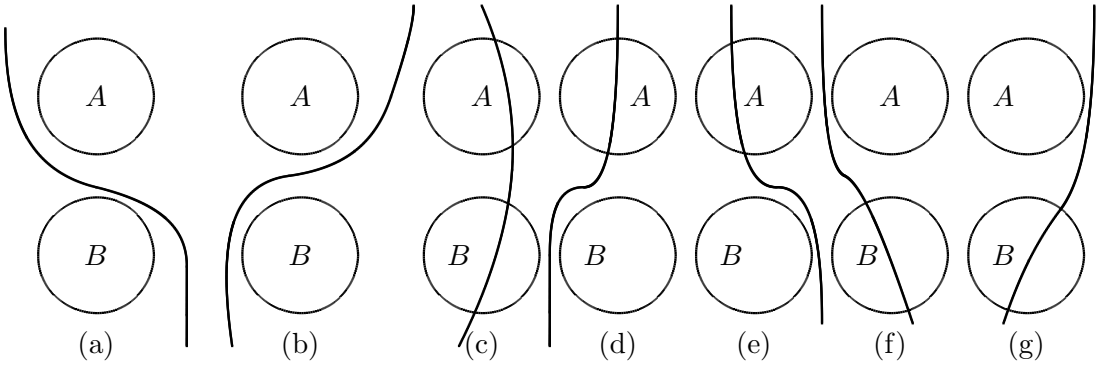

Figure 11. The cut diagrams of a disconnected diagram.

We begin by analyzing the left hand side of the Cutkosky rules. Let T_A and T_B denote the T-matrix associated with individual blobs and T_{AB} denote the T-matrix associated with the combined diagram. If A has n_A disconnected components and B has n_B disconnected components, then according to (2.6) A carries an extra factor of i^{1-n_A} and B carries an extra factor of i^{1-n_B}, while the combined amplitude carries an extra factor of $i^{1-n_A-n_B}$. Therefore we need to remove a factor of i from the product $T_A \otimes T_B$ to get the combined amplitude T_{AB}. This gives

$$T_{AB} = -i\, T_A \otimes T_B\,. \tag{5.38}$$

We define the amplitudes A and B associated with the two blobs as the matrix elements of T_A and T_B between external states. We now see using (5.38) that the combined amplitude is given by $-iAB$. Using the shorthand notation A^* and B^* for hermitian conjugates of A and B we get the left hand side of the Cutkosky rules, encoding the anti-hermitian part of the full amplitude, to be

$$-iAB - (iA^*B^*) = -i(AB + A^*B^*)\,. \tag{5.39}$$

The right hand side of the Cutkosky rules is given by the sum over all the cut diagrams of the original diagram. These are shown in figure 11. The phases of different cut diagrams must be chosen such that the sum over cut diagrams represent matrix elements of $-iT^\dagger T$. However now in T we also need to include the terms $T_A \otimes I_B$ and $I_A \otimes T_B$ besides T_{AB} given in (5.38). Therefore the total relevant contribution to T is given by

$$T = T_A \otimes I_B + I_A \otimes T_B - i\, T_A \otimes T_B\,. \tag{5.40}$$

We can now compare different terms in figure 11 with the corresponding terms in $-iT^\dagger T$ to determine their phases. For example figure 11(a) represents the matrix element of $-i(T_A \otimes I_B)^\dagger (I_A \otimes T_B) = -iT_A^\dagger \otimes T_B$, and hence gives the contribution $-iA^*B$. Similarly figure 11(b) gives the contribution $-iAB^*$. In order to evaluate the contribution from figure 11(c) including its phase we note that this diagram should represent the matrix element of

$$-i(-iT_A \otimes T_B)^\dagger (-iT_A \otimes T_B) = -i(T_A^\dagger T_A) \otimes (T_B^\dagger T_B) = i(T_A - T_A^\dagger) \otimes (T_B - T_B^\dagger), \tag{5.41}$$

JHEP10(2016)024

where in the last step we have used the fact that the blobs A and B individually satisfy the Cutkosky rules and hence $-iT_A^\dagger T_A$ and $-iT_B^\dagger T_B$ are given respectively by $(T_A - T_A^\dagger)$ and $(T_B - T_B^\dagger)$. The matrix element of (5.41) gives $i(A-A^*)(B-B^*)$. Following similar logic we get the contributions from figure 11(d), (e), (f) and (g) to be, respectively, $i(A-A^*)B^*$, $-i(A-A^*)B$, $iA^*(B-B^*)$ and $-iA(B-B^*)$. The last four terms add up to $-2i(A-A^*)(B-B^*)$. Therefore the total contribution to the right hand side of the Cutkosky rules is given by[12]

$$-iA^*B - iAB^* + i(A-A^*)(B-B^*) - 2i(A-A^*)(B-B^*) = -i(AB + A^*B^*). \qquad (5.42)$$

This is in perfect agreement with the left hand side of the Cutkosky rules given in (5.39).

5.4 Mass and wave-function renormalization

In the derivation of the Cutkosky rules we have given, the momentum k carried by a cut propagator is forced to satisfy $k^2 + m^2 = 0$ where m is the tree level mass of the scalar field. However in general a theory of the kind we have analyzed will have finite mass renormalization and hence the constraint on the cut propagator should have been that $k^2 + m_p^2 = 0$ where m_p is the renormalized physical mass. In our analysis this issue shows up in the fact that if we have self energy insertions on a cut propagator on either side of the cut, we get extra propagator factors proportional to $(k^2+m^2)^{-1}$ which diverge. Therefore the Cutkosky rules become only formal relations.

This problem can be avoided by the usual trick of reorganizing Feynman diagrams at each order in perturbation theory. If m_p is the physical mass computed to a given order in perturbation theory, and Z is the wave-function renormalization factor so that the two point function has a pole at $k^2 = -m_p^2$ with residue $-i\,Z$, then for computing any amplitude at higher order, we change k^2+m^2 to $Z^{-1}(k^2+m_p^2)$ in (2.1) and compensate for it by adding to the two point vertex $V^{(2)}$ a new term proportional to $(m^2 - m_p^2) + (1-Z^{-1})(k^2+m_p^2)$. This makes the propagator $-i\,Z\,(k^2+m_p^2)^{-1}$. Now the cut propagator will set $k^2 + m_p^2$ to zero, and the self energy insertions on the cut propagators, after including the contribution from the new two point vertex, will vanish at $k^2 + m_p^2 = 0$. This makes the contribution from the cut diagrams manifestly finite.

Note that the new contribution to $V^{(2)}$ does not carry the exponential suppression factor that was assumed to be present for all $V^{(n)}$. However whenever this new vertex is inserted into an internal propagator of a loop diagram carrying momentum k, there will be some other vertex whose external line carries the same momentum k and hence exponentially suppresses the integrand in the large k^2 region. Therefore the new two point vertex does not affect the ultraviolet finiteness property of individual Feynman diagrams.

[12]Note that two other contributions given by $-i(T_A^\dagger T_A)\otimes I_B$ and $I_A \otimes (-iT_B^\dagger T_B)$ are present in the expressions for $-iT^\dagger T$, but are not included in figure 11. They represent diagrams where either the blob B or the blob A are replaced by forward scattering amplitudes. They will reproduce the anti-hermitian parts of the first two terms on the right hand side of (5.40).

JHEP10(2016)024

6 Field theory model to superstring field theory

We shall now discuss what is involved in going from the toy model we have analyzed to the full string field theory. This discussion will be divided into two parts. In the first part we shall describe generalizations of our analysis to more general quantum field theories, and in the second part we shall turn to the specific case of string field theory.

6.1 More general quantum field theories

In this subsection we shall describe the extension of our analysis to more general class of quantum field theories.

1. *Multiple fields of higher spin.* The toy model of section 2 has only one scalar field. This can be easily generalized to the case of multiple fields including those carrying higher spins and also complex fields. If we denote the complex conjugate of a field ϕ_α by $\phi_{\bar\alpha}$ then the reality condition on the vertices $V^{(n)}_{\alpha_1\cdots\alpha_n}$ and the propagator $P_{\alpha\beta}$ appearing in (2.7) take the form

$$(V^{(n)}_{\alpha_1\cdots\alpha_n}(p_1,\cdots p_n))^* = V^{(n)}_{\bar\alpha_1\cdots\bar\alpha_n}(-p_1^*,\cdots -p_n^*), \quad P_{\alpha\beta}(k)^* = P_{\bar\alpha\bar\beta}(-k^*)\,. \tag{6.1}$$

   For fermions some more signs are needed that will be discussed separately. Now we can proceed with our analysis of section 2.3 as before. The main change is in the fact that in relating $\langle b|T|a\rangle$ to $\langle a|T|b\rangle$ we not only need to change the sign of all the external momenta, but also replace all the field labels α_i by $\bar\alpha_i$. In the second step of the analysis in section 2.3, where we relabel the internal momenta by a change of sign, we also relabel the internal indices carried by the vertices and propagators by their conjugates. In the third step the expression for $\langle b|T|a\rangle^*$ can be manipulated using (6.1) to arrive at an expression that is a modification of that of $\langle a|T|b\rangle$ by complex conjugation of each internal and external momenta and replacement of the factor of i accompanying each loop integration by $-i$. In the fourth step we relabel the loop momentum integration variables by their complex conjugates to arrive at an expression in which the integrand is related to that in $\langle a|T|b\rangle$ by the replacement of the external momenta by their complex conjugates, and the integration contour is related to the original one by complex conjugation. Rest of the analysis remains unchanged.

   Typically theories with higher spin fields have gauge symmetries, and as a result not all states propagating in the propagator are physical. In such cases Cutkosky rules do not by themselves imply unitarity — we have to do additional work to show that the unphysical state contribution cancels. There are also massless fields for which our analysis may break down. We shall return to these points when we describe applications to string field theory.

2. *Fermions.* For fermionic fields there are a few additional signs that need to be taken care of. First of all the vertices $V^{(n)}$ are no longer fully symmetric under permutations of fields — under the exchange of a pair of fermionic states they pick up minus

JHEP10(2016)024

signs. Since the complex conjugate of the product of grassmann variables involves reversing their order in the product besides taking conjugates of each variable, in the reality constraint (6.1), the order of the fermionic indices carried by the vertices and propagators on the two sides of the equation will have to be in opposite order leading to extra signs in our analysis. Also the hermitian conjugate of a multi-particle state containing fermions will involve the conjugate states arranged in opposite order. As a result in the analysis of section 2.3, the computation of $\langle b|T|a\rangle$ will now not only involve reversing the signs of the external momenta and complex conjugating the labels of external states, but also changing the order of the fermions in the external states. After performing manipulations similar to that in section 2.3 we arrive at the result that the computation of $T^\dagger$ will involve evaluating an integral whose integrand differs from that of the original integrand for T by complex conjugation of external momenta and

(a) a reversal of the order of the fermionic labels in the external states,

(b) a reversal of the order of the fermionic labels carried by the vertices, and

(c) a reversal of the order of the fermionic labels carried by the propagators.

Let us denote by $2n_e$ the total number of external fermions, by $2n_v$ the total number of fermionic labels carried by the vertices and by n_p the total number of internal fermionic propagators. Then the net factor from the three effects mentioned above is $(-1)^{n_p+n_v+n_e}$. Using the relation $n_v - n_e = n_p$ we see that this number is 1. Therefore we get back the same integrand as that in the computation of T except for complex conjugation of the external momenta. As before the integration contour will be given by the complex conjugate of the integration contour for T.

In subsequent analysis, another set of minus signs originate from the fact that each fermion loop is accompanied by a minus sign. Therefore if we have a cut diagram in which N fermion loops are cut, the diagram is accompanied by a factor of $(-1)^N$. When we attempt to interpret this as a contribution to $T^\dagger T$ by inserting a complete set of states $|\alpha\rangle\langle\alpha|$ between T and $T^\dagger$, then the order of the $2N$ fermions in $|\alpha\rangle$ and $\langle\alpha|$ must be opposite. Reversing the order of the $2N$ fermions leads to another factor of $(-1)^N$ that cancels the $(-1)^N$ factor coming from the N fermion loops.

6.2 String field theory

We shall now describe the implication of our results for string field theory.

1. *Exponential suppression of vertices at large momentum.* The key feature of the toy model of section 2 is the peculiar form of the interaction vertices in the momentum space, possessing an essential singularity at infinity, diverging exponentially as $k^2 \to -\infty$ and falling off exponentially as $k^2 \to \infty$ for any momentum k carried by an external line to the vertex. In string field theory this exponential factor comes from the conformal transformation of the vertex operator. In defining the off-shell vertex we have to choose local coordinate system at the punctures and by scaling the local

JHEP10(2016)024

coordinate at a puncture by some real number β, we can scale the off-shell vertex by a factor of β^h where h is the $L_0+\bar{L}_0$ eigenvalue of the vertex operator. Since $L_0+\bar{L}_0$ has an additive contribution of $k^2/2$ besides the oscillator contribution, this introduces a factor of $\beta^{k^2/2} = \exp[(k^2 \ln \beta)/2]$, and this can be made small for large k^2 by taking β to be small. In the string field theory literature this operation of scaling local coordinates by β is known as the act of adding stubs of length $-\ln \beta$ to the vertices. Physically choosing small β i.e. long stubs amounts to ensuring that integration over most of the moduli space of Riemann surfaces comes from the elementary vertices, and only small regions near the boundary of the moduli space come from Feynman diagrams with internal propagators.

2. *Poles of the propagator.* We have assumed that the only poles of the propagator occur at $k^2+m^2=0$ for different values of m. In string field theory this is automatic in the Siegel gauge.

3. *Infinite number of states.* Since string field theory has infinite number of fields, we also need to ensure that the sum over fields that appear in the evaluation of the Feynman diagrams converge. The number of states below a certain mass m grows as $\exp[c_1 m]$ for some positive constant c_1, and the stubs suppress the vertices by a factor of $\exp[-c_2 m^2]$ for some positive constant c_2 that can be made arbitrarily large. Therefore we expect the sums to be convergent.

4. *Analyticity of the vertices at finite momentum.* In our analysis we have assumed that the interaction vertices are analytic as function of external momenta for finite momenta. In string field theory this is a consequence of the fact that the n-point interaction vertices are obtained as integrals over subspaces of moduli spaces of genus g Riemann surfaces with n-punctures for various values of g, and that *these subspaces never include any degenerate Riemann surface.*

5. *Reality of the action.* In the derivation of the Cutkosky rules we needed to make use of the reality of the action. Therefore to extend the proof to string field theory we need to prove the reality of the string field theory action. This has been proved for the bosonic string theory [36]. It is expected that a similar proof can be given for superstring field theory with judicious choice of the locations of the picture changing operators, but this has not yet been worked out.

6. *Decoupling of unphysical states.* A more serious issue arises from the fact that among the fields of string field theory there are many auxiliary fields, pure gauge fields and ghost fields which do not correspond to physical particles. In the Siegel gauge in which the propagator is proportional to $(L_0+\bar{L}_0)^{-1} = 2(k^2+C)^{-1}$ where $C/2$ gives the discrete contribution to $L_0+\bar{L}_0$ from the oscillators, all the fields contribute to the poles and hence will be summed over as intermediate states in the Cutkosky rules. As a result, Cutkosky rules by themselves do not prove unitarity. The complete proof will involve showing that the contribution from all fields other than the physical fields vanish or cancel. In principle this should be possible with the help of Ward identities of the kind described in [27], but the details need to be worked out.

JHEP10(2016)024

7. *Massless states.* The spectrum of superstring theory contains massless states, and as a result the S-matrix suffers from infrared divergences. Therefore unitarity may not hold in the usual sense. In our analysis this problem shows up in the breakdown of our implicit assumption that at a pinch singularity only one of the two poles in a propagator blows up. For example for $m = 0$ in (3.3), as $\vec{\ell} \to 0$ both poles Q_1 and Q_2 approach the contour from two sides and pinch it at the origin even when all the external energies are taken to be imaginary and the integration contour lies along the imaginary ℓ^0 axis. Since we have worked with fixed values of the spatial components of loop momenta, our analysis can still be used for generic values of these spatial momenta, but will break down when one or more internal or external massless particle carries zero spatial momenta. In sufficiently large dimensions (> 4) configurations with zero spatial momenta do not contribute to T or $T^\dagger T$ due to the vanishing of the integration measure dominating the divergences from the propagators. In such cases infrared divergences are tame and our result holds. In dimensions ≤ 4 we need to be more careful — work with cross section instead of S-matrix and sum over final states and average over initial states [35, 37–39]. Since our proof of Cutkosky rules holds for fixed spatial components of loop momenta, we expect that the method described in [35] can be used to prove finiteness of appropriate inclusive cross sections after averaging over initial states, but the details need to be worked out.

8. *Vacuum shift.* Like in ordinary quantum field theories, in string field theory the vacuum can get shifted from the original classical vacuum by vacuum expectation values of certain fields. Since the interaction vertices around the shifted vacuum have the same analytic structure as in the original vacuum, the Cutkosky rules will hold in the new vacuum as well. This of course requires that the fields acquiring vacuum expectation values satisfy appropriate reality condition so that the action expanded around the new vacuum continues to be real.

9. *Mass renormalization.* Massive particles in string theory undergo mass renormalization. The S-matrix has to be defined by taking into account these effects. We expect that the proof of unitarity can be carried through even in the presence of these effects following the same steps as in section 5.4. There is also the issue that most of the massive particles in string theory become unstable under quantum corrections and hence cease to be true candidates for asymptotic states. We expect that this effect can also be taken into account following the same method as in a quantum field theory [24].

Therefore the two main technical problems that need to be solved before we can declare superstring field theory amplitudes to be unitary are:

1. proving reality of the superstring field theory action, and

2. showing that the contribution to the cut propagator from the unphysical and pure gauge states cancel, leaving behind only the contribution from physical states.

JHEP10(2016)024

Acknowledgments

We wish to thank Corinne de Lacroix, Eric D'Hoker, Harold Erbin, George Sterman and Edward Witten for useful discussions. The research of R.P. was supported in part by Perimeter Institute for Theoretical Physics. Research at Perimeter Institute is supported by the Government of Canada through Industry Canada and by the Province of Ontario through the Ministry of Research and Innovation. This research of A.S. was supported in part by the DAE project 12-R&D-HRI-5.02-0303 and J.C. Bose fellowship of the Department of Science and Technology, India.

JHEP10(2016)024

References

[1] A. Sen, *BV Master Action for Heterotic and Type II String Field Theories*, *JHEP* **02** (2016) 087 [arXiv:1508.05387] [INSPIRE].

[2] E. Witten, *Interacting Field Theory of Open Superstrings*, *Nucl. Phys.* **B 276** (1986) 291 [INSPIRE].

[3] R. Saroja and A. Sen, *Picture changing operators in closed fermionic string field theory*, *Phys. Lett.* **B 286** (1992) 256 [hep-th/9202087] [INSPIRE].

[4] N. Berkovits, *SuperPoincaré invariant superstring field theory*, *Nucl. Phys.* **B 450** (1995) 90 [*Erratum ibid.* **B 459** (1996) 439] [hep-th/9503099] [INSPIRE].

[5] N. Berkovits, *The Ramond sector of open superstring field theory*, *JHEP* **11** (2001) 047 [hep-th/0109100] [INSPIRE].

[6] Y. Okawa and B. Zwiebach, *Heterotic string field theory*, *JHEP* **07** (2004) 042 [hep-th/0406212] [INSPIRE].

[7] N. Berkovits, Y. Okawa and B. Zwiebach, *WZW-like action for heterotic string field theory*, *JHEP* **11** (2004) 038 [hep-th/0409018] [INSPIRE].

[8] T. Erler, S. Konopka and I. Sachs, *Resolving Witten's superstring field theory*, *JHEP* **04** (2014) 150 [arXiv:1312.2948] [INSPIRE].

[9] H. Kunitomo, *The Ramond Sector of Heterotic String Field Theory*, *PTEP* **2014** (2014) 043B01 [arXiv:1312.7197] [INSPIRE].

[10] T. Erler, S. Konopka and I. Sachs, *NS-NS Sector of Closed Superstring Field Theory*, *JHEP* **08** (2014) 158 [arXiv:1403.0940] [INSPIRE].

[11] H. Matsunaga, *Nonlinear gauge invariance and WZW-like action for NS-NS superstring field theory*, *JHEP* **09** (2015) 011 [arXiv:1407.8485] [INSPIRE].

[12] H. Kunitomo, *Symmetries and Feynman rules for the Ramond sector in open superstring field theory*, *PTEP* **2015** (2015) 033B11 [arXiv:1412.5281] [INSPIRE].

[13] T. Erler, Y. Okawa and T. Takezaki, A_∞ *structure from the Berkovits formulation of open superstring field theory*, arXiv:1505.01659 [INSPIRE].

[14] T. Erler, S. Konopka and I. Sachs, *Ramond Equations of Motion in Superstring Field Theory*, *JHEP* **11** (2015) 199 [arXiv:1506.05774] [INSPIRE].

[15] K. Goto and H. Matsunaga, *On-shell equivalence of two formulations for superstring field theory*, arXiv:1506.06657 [INSPIRE].

[16] S. Konopka, *The S-matrix of superstring field theory*, *JHEP* **11** (2015) 187 [arXiv:1507.08250] [INSPIRE].

[17] H. Kunitomo and Y. Okawa, *Complete action for open superstring field theory*, *PTEP* **2016** (2016) 023B01 [arXiv:1508.00366] [INSPIRE].

[18] K. Goto and H. Matsunaga, *A_∞/L_∞ structure and alternative action for WZW-like superstring field theory*, arXiv:1512.03379 [INSPIRE].

[19] T. Erler, Y. Okawa and T. Takezaki, *Complete Action for Open Superstring Field Theory with Cyclic A_∞ Structure*, *JHEP* **08** (2016) 012 [arXiv:1602.02582] [INSPIRE].

[20] S. Konopka and I. Sachs, *Open Superstring Field Theory on the Restricted Hilbert Space*, *JHEP* **04** (2016) 164 [arXiv:1602.02583] [INSPIRE].

[21] B. Jurčo and K. Muenster, *Type II Superstring Field Theory: Geometric Approach and Operadic Description*, *JHEP* **04** (2013) 126 [arXiv:1303.2323] [INSPIRE].

[22] R.E. Cutkosky, *Singularities and discontinuities of Feynman amplitudes*, *J. Math. Phys.* **1** (1960) 429 [INSPIRE].

[23] M. Fowler, *Introduction to Momentum Space Integration Techniques in Perturbation Theory*, *J. Math. Phys.* **3** (1962) 936.

[24] M.J.G. Veltman, *Unitarity and causality in a renormalizable field theory with unstable particles*, *Physica* **29** (1963) 186 [INSPIRE].

[25] G. 't Hooft and M.J.G. Veltman, *Diagrammar*, *NATO Sci. Ser.* **B 4** (1974) 177 [INSPIRE].

[26] S. Bloch and D. Kreimer, *Cutkosky Rules and Outer Space*, arXiv:1512.01705 [INSPIRE].

[27] A. Sen, *Supersymmetry Restoration in Superstring Perturbation Theory*, *JHEP* **12** (2015) 075 [arXiv:1508.02481] [INSPIRE].

[28] K. Aoki, E. D'Hoker and D.H. Phong, *Unitarity of Closed Superstring Perturbation Theory*, *Nucl. Phys.* **B 342** (1990) 149 [INSPIRE].

[29] E. Witten, *Superstring Perturbation Theory Revisited*, arXiv:1209.5461 [INSPIRE].

[30] R. Donagi and E. Witten, *Supermoduli Space Is Not Projected*, *Proc. Symp. Pure Math.* **90** (2015) 19 [arXiv:1304.7798] [INSPIRE].

[31] R. Donagi and E. Witten, *Super Atiyah classes and obstructions to splitting of supermoduli space*, arXiv:1404.6257 [INSPIRE].

[32] A. Sen and E. Witten, *Filling the gaps with PCO's*, *JHEP* **09** (2015) 004 [arXiv:1504.00609] [INSPIRE].

[33] A. Berera, *Unitary string amplitudes*, *Nucl. Phys.* **B 411** (1994) 157 [INSPIRE].

[34] E. Witten, *The Feynman $i\epsilon$ in String Theory*, *JHEP* **04** (2015) 055 [arXiv:1307.5124] [INSPIRE].

[35] G.F. Sterman, *An Introduction to quantum field theory*, Cambridge University Press (1993).

JHEP10(2016)024

[36] B. Zwiebach, *Closed string field theory: Quantum action and the B-V master equation*, *Nucl. Phys.* **B 390** (1993) 33 [hep-th/9206084] [INSPIRE].

[37] T. Kinoshita, *Mass singularities of Feynman amplitudes*, *J. Math. Phys.* **3** (1962) 650.

[38] T.D. Lee and M. Nauenberg, *Degenerate Systems and Mass Singularities*, *Phys. Rev.* **133** (1964) B1549.

[39] F. Bloch and A. Nordsieck, *Note on the Radiation Field of the electron*, *Phys. Rev.* **52** (1937) 54 [INSPIRE].

JHEP10(2016)024